NASA Contractor Report 179612

DESIGN AND ANALYSIS REPORT FOR THE FLIGHT WEIGHT 20-INCH COLUMBIUM SECONDARY NOZZLE FOR THE RL10 ENGINE

FINAL REPORT

Pratt & Whitney
Government Engine Business
P.O. Box 109600
West Palm Beach, Florida 33410-9600

February 1989

NASA

National Aeronautics and
Space Administration

FOREWORD

This document presents the design and analysis of the flight weight 20-inch columbium secondary nozzle for the RL10 engine, performed under Contract NAS3-24238 (C.O. T. P. Burke). This study was conducted for the National Aeronautics and Space Administration — Lewis Research Center (NASA-LeRC) by Pratt & Whitney (P&W). Mr. R.R. Foust was the engineering manager for this effort with Mr. J. H. Castro as the principal investigator and author of this report.

PRECEDING PAGE BLANK NOT FILMED

$\mathcal{I}, \mathbb{I}$

3097C

3105C

(Continued)

3105C

LIST OF ILLUSTRATIONS

LIST OF ILLUSTRATIONS (Continued)

SECTION I
INTRODUCTION

Pratt & Whitney (P&W) is currently under contract to NASA-LeRC for a multi-year program to evaluate the feasibility of the RL10-IIB/IIC engine models and the various improvements which broaden the engine capabilities and range of applications. The program is funded under NASA Contracts NAS3-22902, NAS3-24238 and NAS3-24738, and is entitled "The RL10 Product Improvement Program" (PIP). It provides a sound basis for the selection of features which could be included in an engine for a cryogenic rocket upper stage.

The features being evaluated include the operation of the RL10 engine at low thrust levels and/or high mixture ratio levels and the addition of a translating nozzle to the engine to increase its specific impulse while shortening the installed engine length. The addition of a translating nozzle also requires the recontour of the engine thrust chamber to optimize the expansion of the products of combustion to the larger area ratio (ε). When all of the above features are incorporated into the existing RL10 engine the result is the RL10-IIB derivative engine. The RL10-IIC engine model differs from the RL10-IIB in that it does not have the low thrust operational capability. The translating nozzle for the RL10-IIB/IIC engine is approximately 55 inches in length with an exit plane diameter of 71 inches and an inlet plane diameter of 40 inches. The RL10-IIB/IIC engine is illustrated in Figure 1.

Due to the unavailability of a test site to accommodate the large exit-plane-diameter translating nozzle and the fact that the recontoured thrust chamber would not be available until 1985, it was decided early in the program to fabricate a small subscale carbon/carbon (c/c) nozzle. This nozzle could be fitted to an existing RL10A-3-3A thrust chamber and tested in P&W test facilities. By testing a c/c nozzle in the RL10 exhaust environment early in the program, the feasibility of the nozzle concept could be proven. The findings from the test series could then be incorporated into the nozzle final design for the RL10-IIB/IIC engine.

Two 20-inch carbon/carbon nozzles were fabricated and tested in the RL10 engine during the 1984-1985 time period. At the time of this report the first nozzle has accumulated 5671 seconds of running time in 45 starts while the second nozzle suffered a test stand induced failure during engine shutdown after accumulating 3562 seconds of running time in 24 starts (Ref. 2)

As a backup to the carbon/carbon nozzle design, a Centaur compatible, flight weight, refractory metal (columbium) nozzle was designed. The design and analysis of this nozzle is presented in this report.

As in the c/c nozzles, this columbium nozzle was designed to fit the extended contour of the existing RL10A-3-3A engine. The nozzle exit plane diameter (approximately 46 inches) is limited by the maximum diameter that the test facility could accommodate. The length of the subscale nozzle (20 inches) is the result of the intersection of the 46 inch exit plane diameter with the predetermined nozzle contour (Ref. 1). A nozzle exit plane diameter of 46 inches can also be accommodated in a twin engine centaur vehicle without significant change.

This report provides a discussion of the flight weight 20-inch columbium nozzle design. Figure 2 illustrates the flight weight 20-inch columbium nozzle installed in the RL10A-3-3A engine. With the nozzle in the stowed position, the engine is 70 inches long (ε = 61:1); with the nozzle deployed, the engine length and area ratio are increased to 90 inches and 83:1, respectively. The increase in area ratio provides an additional estimated 7 ± 1 seconds of specific impulse. The flight weight 20-inch columbium nozzle is scheduled to be tested by P&W during the summer of 1987.

1
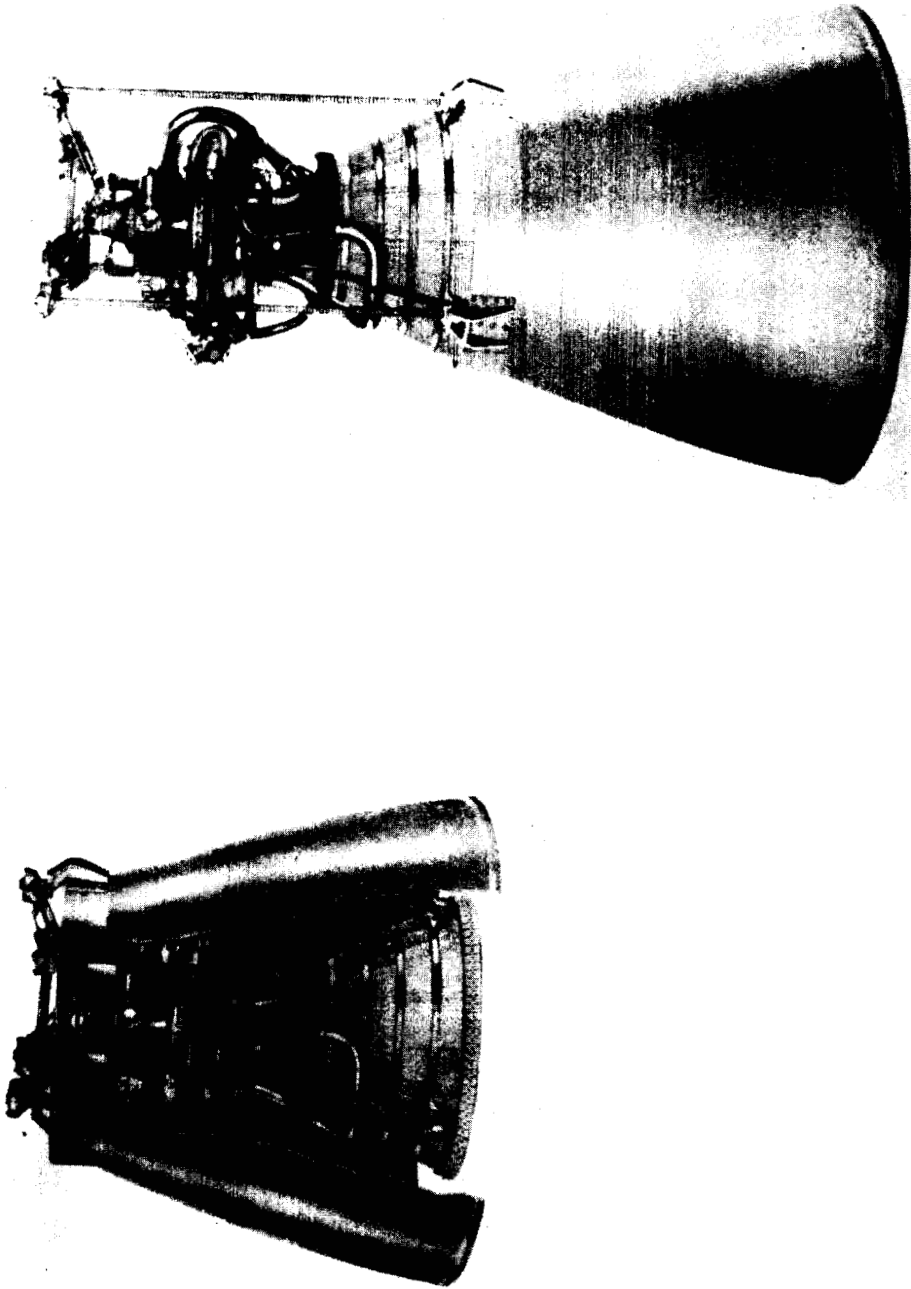
FD 278867

Nozzle in Deployed Position

Figure 1. *RL10 Derivative IIB/IIC Engine-Nozzle Extension*

4528C
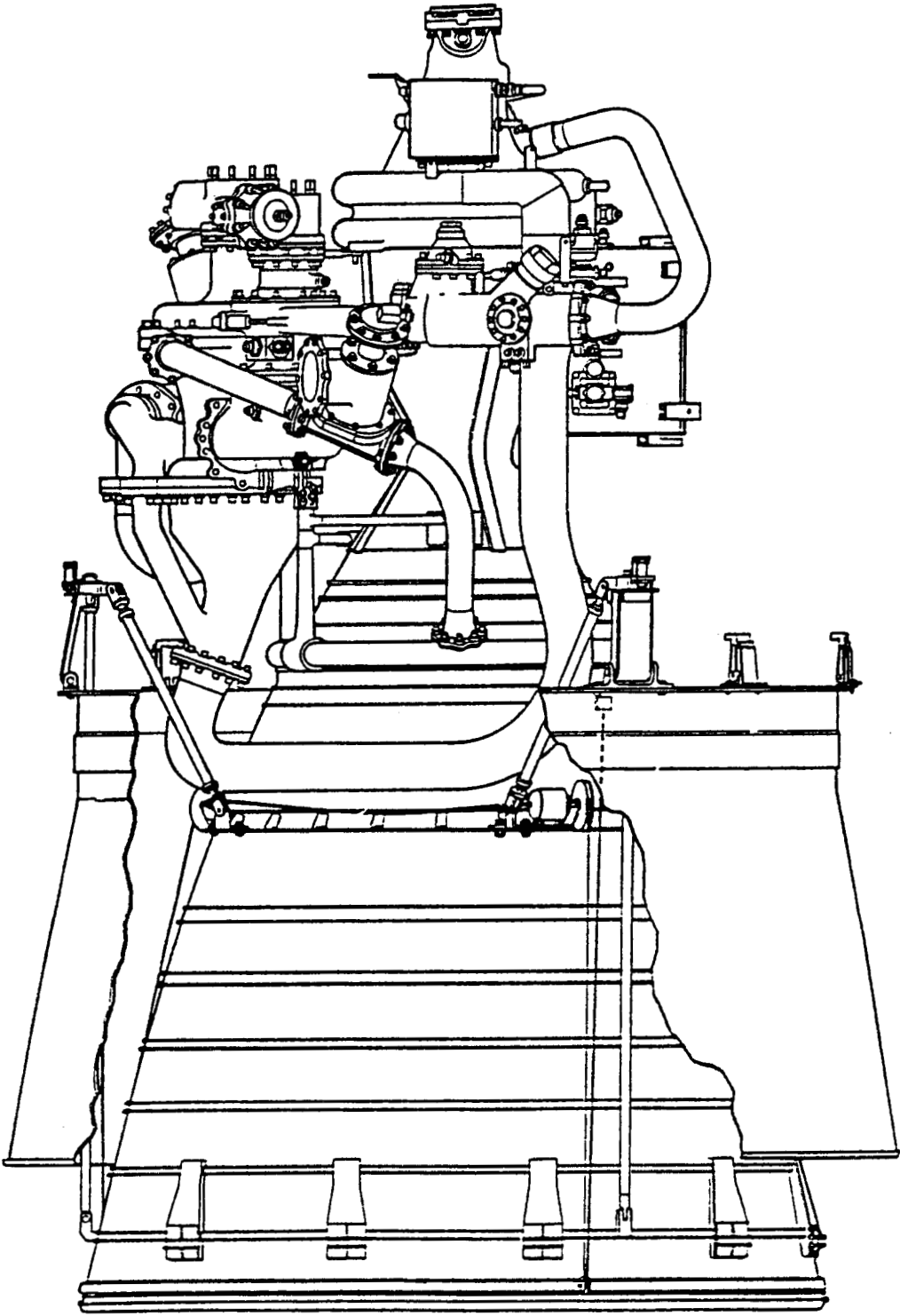
FD 328016

Figure 2.   Flight Weight 20-Inch Columbium Nozzle in the RL10A-3-3A Engine

SECTION II
FLIGHT WEIGHT TWENTY-INCH COLUMBIUM NOZZLE DESIGN

The design of the flight weight 20-inch columbium nozzle was initiated at the request of NASA as a backup for the 20-inch carbon/carbon nozzle design. The flight weight 20-inch columbium nozzle is to have the same contour as the 20-inch carbon/carbon nozzle but will differ from the carbon/carbon nozzle in material and was design optimized for minimum weight. Columbium was chosen as the nozzle material for its high temperature environment capability and because it has been widely used by the Aerospace Industry for other rocket nozzle applications.

The WC103 columbium alloy (Co-10Hf-1Ti) was selected because of its adequate temperature/strength capability for the nozzle application, its manufacturability, and its wide availability (compared to other columbium alloys). Since it is currently in use in the F100 gas turbine engine, P&W has a large experience base in the use of this alloy.

The design of the flight weight 20-inch columbium nozzle (referred to herein as the 20-inch Cb nozzle) was conducted on two iterations. The first iteration, shown in Figure 3, was designed using the test stand shutdown loads previously used for the 20-inch carbon/carbon nozzle design. These loads were redefined after the Low Pressure Impregnation (LPI) densified c/c nozzle failure (Ref. 2), which rendered the original 20-inch Cb nozzle design obsolete. Additionally, the original design was not optimized for fabricability which made it expensive to produce.
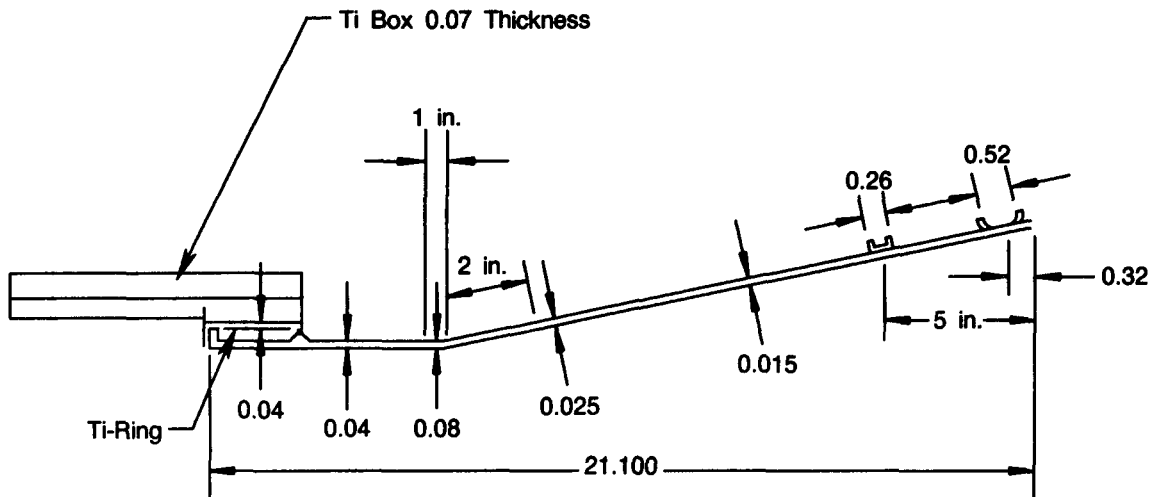
FDA 329873

Figure 3. Original 20-inch Flight Weight Columbium Nozzle Design

The second 20-inch Cb nozzle design iteration incorporated the more severe, redefined, shutdown loads and manufacturer's suggestions to optimize the design for fabricability and reduce its cost. This second design iteration will be discussed in this report. At the time of the second iteration, the 20-inch Cb nozzle was directed by NASA to become the primary material approach, relegating the carbon/carbon design to the backup position.

The 20-inch Cb nozzle installation is shown in Figure 4. The nozzle is attached to the RL10 primary chamber through a system of 12 titanium spring-loaded latches and three aluminum

4

guide rods. The latch and support system will be discussed in detail in Section III of this report. The nozzle is fabricated from C-103 columbium (PWA 1095) material. It mates with an AMS 4928 titanium ring at its forward end. This ring is used to stiffen the nozzle front end and allows for attachment to the RL10 primary nozzle. A much larger removable stiffening ring is prominent in Figure 4. This ring, made of 6061-T6 aluminum, is designed to also stiffen the nozzle front end and react the shutdown loads that dominate the nozzle design. The ring is only intended to be used during ground testing since the engine doesn't experience the test stand induced shutdown spike during flight. The ring is a box-like structure 7.0 inches high by 4.0 inches deep with an inside diameter of 44.0 inches and a ring wall thickness of 0.100 inch. The box structure incorporates stiffening webs along the circumference of the ring. The ring is divided into two identical 180-degree segments for ease of carrying and installation, and bolts to the nozzle titanium ring through a set of stainless steel brackets.

The 20-inch Cb nozzle assembly dimensions are shown in Figure 5. The nozzle is approximately 21 inches in length and ranges in thickness from 0.051 inch minimum at its front to 0.042 minimum and 0.027 minimum in its mid section to 0.017 inch minimum at the aft section. The nozzle exit plane is stiffened by a 0.380 inch high, 0.027 inch minimum thickness stiffening ring. The thickness minimum dimensions are before coating so that the nozzle can carry the design loads. During the coating process 0.001 inch per side of the nozzle will be consumed by the diffusion of the coating into the substrate material. The upper end of the dimensional tolerance on the nozzle is controlled by providing a maximum nozzle weight before coating. For the nozzle detail this maximum weight is 27.7 lb.

The complete nozzle assembly including the riveted titanium ring, but without the removable aluminum ring, weighs 36.8 lb.

Over 2½ hours of carbon/carbon nozzle testing has documented the 7 ± 1 seconds of specific impulse (I_{sp}) increase attributed to the nozzle.

5
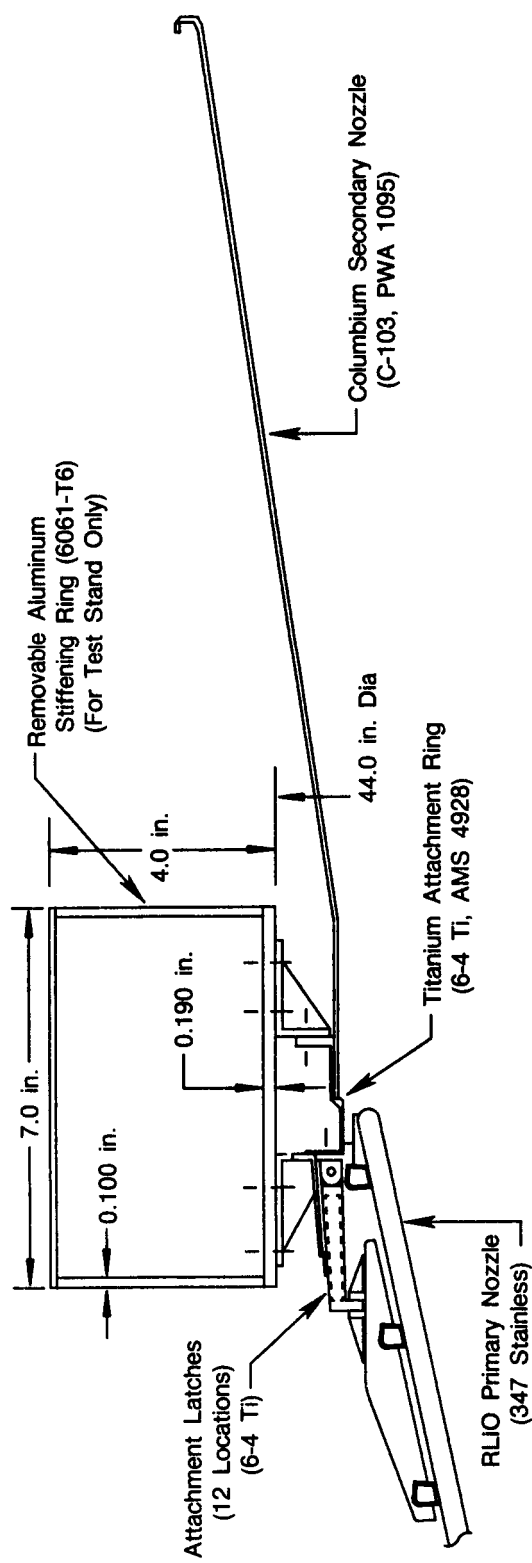
Figure 4. Flight Weight 20-inch Columbium Nozzle Installation

FDA 329867

Removable Aluminum
Stiffening Ring (6061-T6)
(For Test Stand Only)

Columbium Secondary Nozzle
(C-103, PWA 1095)

44.0 in. Dia

Titanium Attachment Ring
(6-4 Ti, AMS 4928)

4.0 in.

7.0 in.

0.190 in.

0.100 in.

Attachment Latches
(12 Locations)
(6-4 Ti)

RL1O Primary Nozzle
(347 Stainless)

6
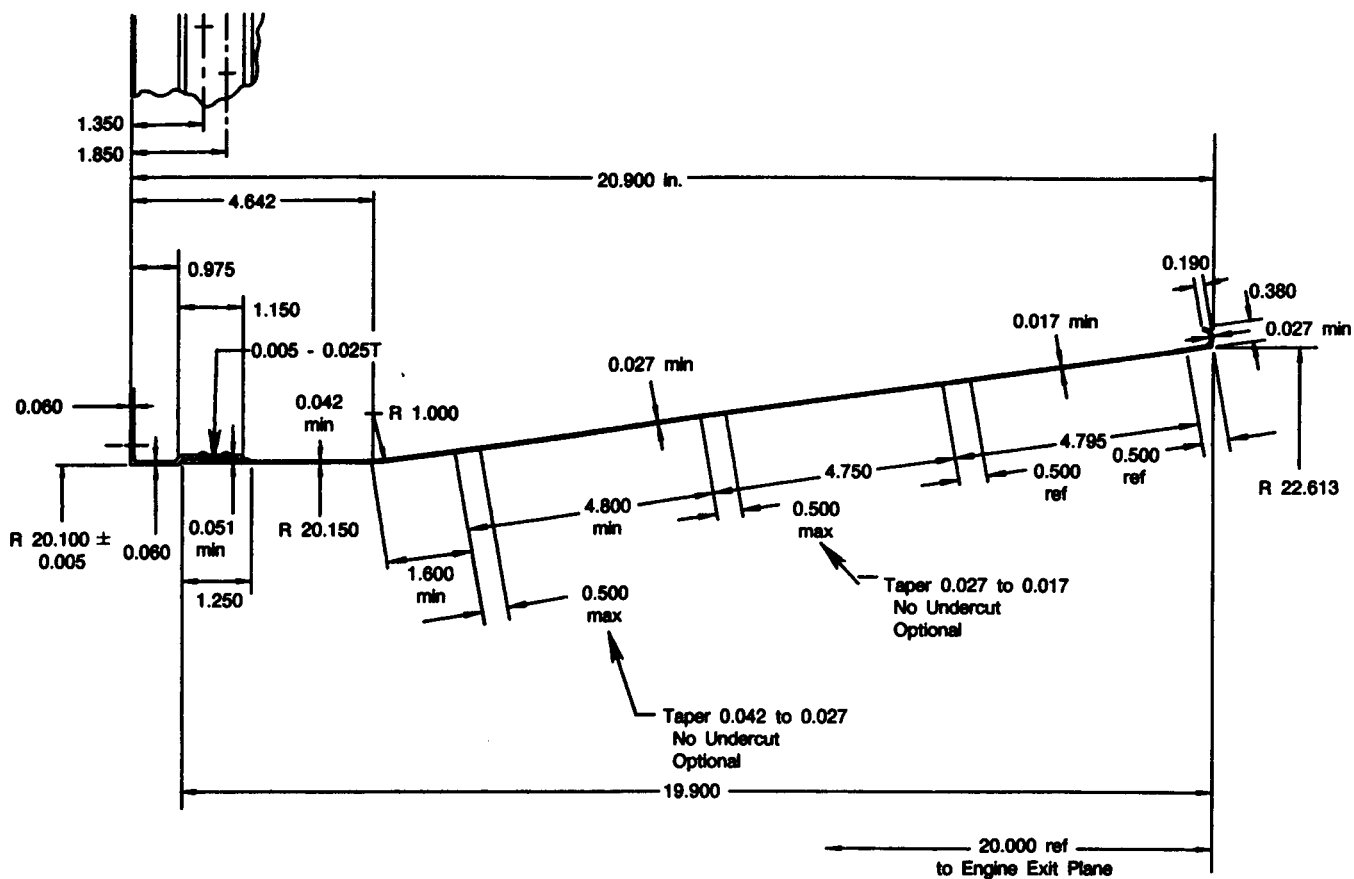
Figure 5. Flight Weight 20-inch Columbium Nozzle Dimensions

7

SECTION III
FLIGHT WEIGHT 20-INCH NOZZLE LATCHING AND SUPPORT HARDWARE DESIGN

For this report, the nozzle support and latching system will be divided into three separate sections: the nozzle guide rods, nozzle latches, and nozzle seal.

A. NOZZLE GUIDE RODS

As in the jackscrew actuation/nozzle support system, described in Ref. 1, the flight weight system design consists of three nozzle rods equally spaced around the circumference of the engine. These rods are not threaded as in the previous design, but rather have smooth surfaces on which three sliding brackets, attached to the nozzle titanium ring, ride. The three rods (guide rods) act as guides on which the nozzle assembly rides during its translation from the stowed to the deployed position. For weight saving purposes, the guide rods are fabricated from thin wall aluminum tubing. For anti-frictional purposes the guide rods are coated with TUFRAM®, a hard, self-lubricating coating widely used on aluminum. A typical guide rod installation is shown in Figure 6.

The front end of the guide rod is supported by a bracket which connects to the RL10 chamber through two adjustable tie rods (for alignment) which bolt to one of the chamber reinforcement bands. This system is similar to the one used in the carbon/carbon nozzle design (Ref. 1) except that it has been optimized for weight reduction. The guide rod front-end support is illustrated in Figure 6.

The aft end of the nozzle guide rod is attached to the chamber through a pin joint to a support bracket which is welded into the second from the last aft end reinforcing band of the RL10 chamber. The aft support of the guide rod is also shown in Figure 6.

The guide rods are designed to accommodate different actuation systems ranging from electric motors to spring motors to lanyards. A number of these systems have been evaluated but no selection has been made to date.

B. LATCHING SYSTEM

The flight weight latching system consists of 12 titanium (AMS 4928) finger latches and their corresponding sockets, mounted equally spaced around the circumference of the engine. Each of the latches is spring loaded to the locked position by a flat spring which is riveted to the latch support bracket. The rotating section of each latch is pinned to a latch support bracket which is in turn bolted to the flight weight nozzle titanium ring (see Figure 7). The latch socket is riveted to a socket support bracket which is welded to two of the thrust chamber reinforcing bands.

An optimization study was made to determine the size and number of latches versus weight added to the engine including the nozzle extension. This study concluded that the minimum weight could be achieved by utilizing 25-30 small latches. During structural analysis it was found that this essentially complete circumferential tie between the two nozzles causing stresses in the primary nozzle in excess of yield during shutdown loadings. Modifications to the nozzle extension and latching system, and further analysis in attempts to find a solution to this problem, showed that substantial weight would have to be added to the nozzle extension.

8

FD 329869

Flight Weight
20 - inch
Cb Nozzle
in Extended
Position
(PWA1095)

Chamber

Pin

Joint

Titanium
Reinforcing Ring

Tie Rod
Assemblies

30 deg Typ

10 deg Ref

(AMS 4082)
Guide Rod

Nozzle Extension

Nozzle
Latches
(typ)

Engine Vertical
℄ Reference

Nozzle
Sliding
Bracket
(AMS 4027)

Required Nozzle
Translation - 21 in. Min

RL10
Thrust
Chamber / Primary Nozzle

RL10
Thrust
Chamber
Reinforcing
Band

Tie Rod
Assy (AMS 4082)

Existing Chamber
Reinforcing Band

Stowed Position of
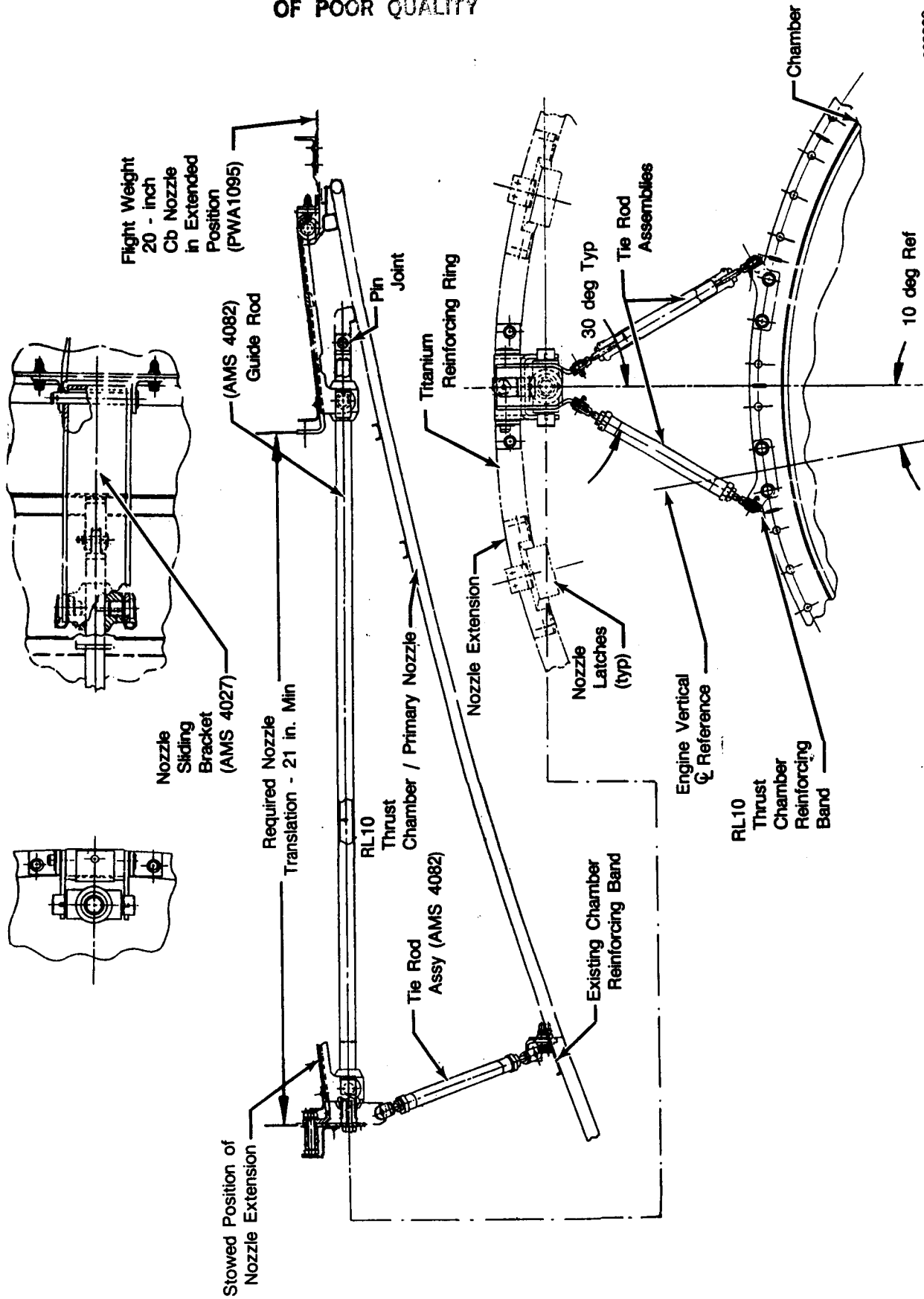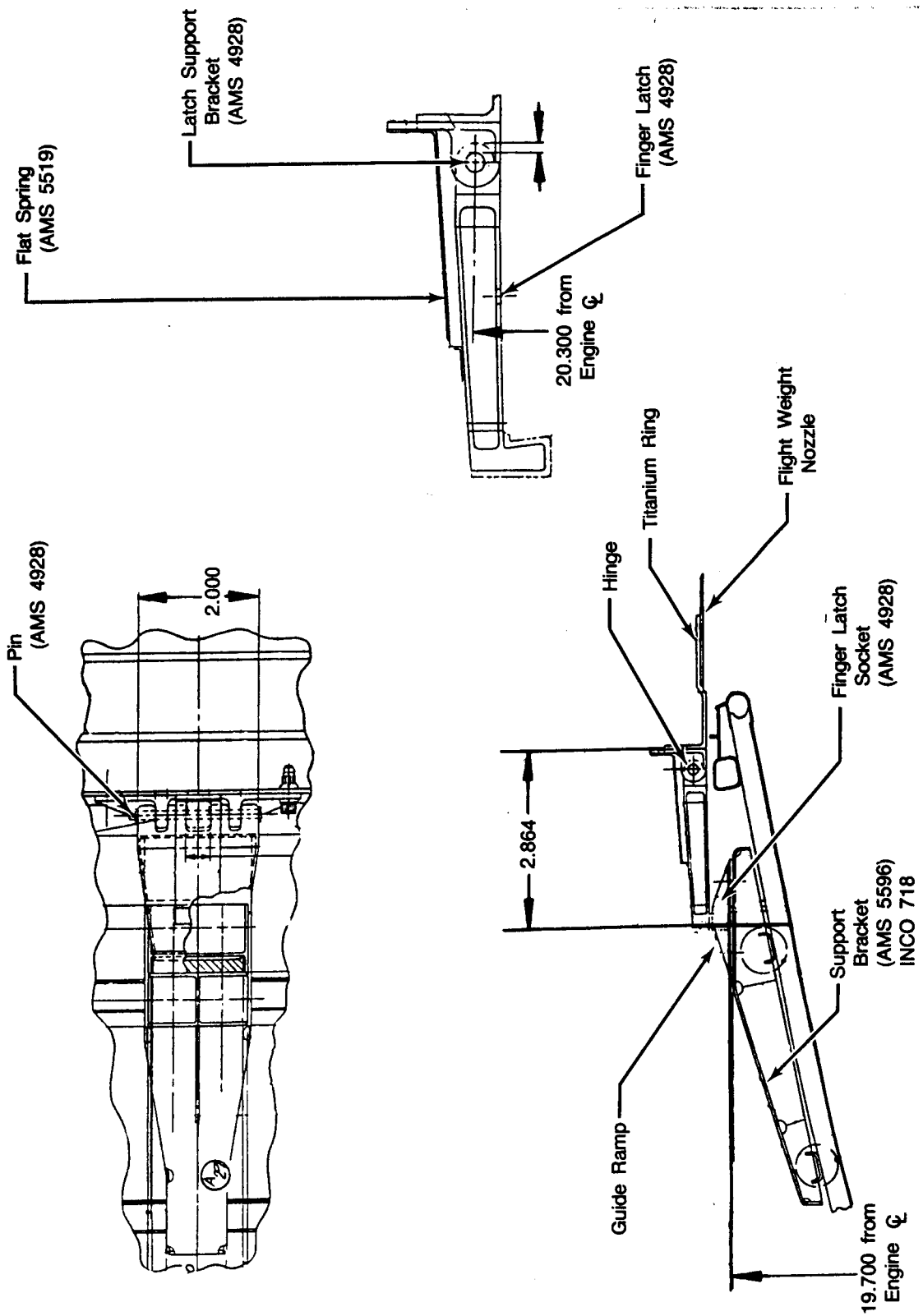Nozzle Extension

Figure 6. Nozzle Guide Rod Installation in RL10 Engine

9

Figure 7. Flight Weight Nozzle Latching System

FD 329870

10

3097C

A change in RL10 ground testing philosophy was mandated by this unacceptable weight penalty. It was decided that the reinforcement ring previously described in Section II should be added to the nozzle extension during ground test to stiffen the forward end thus reducing the loads on the primary nozzle. This stiffener also allowed a reduction in the number of latches from 27 to 12. As previously explained, this ring is only intended for ground test and will be removed for flight.

To minimize weight, all bolted-on hardware is fabricated of AMS 4928 titanium or 6061-T6 aluminum. All hardware welded to the chamber is made of 374 SST with the exception of the socket mounting bracket which is INCO 718 to minimize deflection. A minimum margin of safety of 0.5 has been maintained in all latching system hardware and a margin of 1.7 has been achieved in the primary nozzle. These margins are for test stand shutdown loadings. Flight loads yield much higher margins.

Like the guide rod support system, the finger latching system can be used with a number of different nozzle actuation mechanisms. The operation of the latches is simple in nature. As the nozzle is extended, the foot of the finger latch rides up a self-aligning ramp, located in the forward portion of the latch socket. The force exerted by the ramp rotates the finger assembly about the pivot pin and against the force of the flat spring. When the foot of the latch is aligned with the socket, the flat spring forces the foot into the socket, locking the nozzle in place.

The latch sockets were designed to provide axial and circumferential restraint to the finger latches. This requirement was brought about by the eccentric nature of the shutdown loads that the nozzle was designed to withstand.

C. NOZZLE SEAL

The experience obtained during the Product Improvement Program (PIP) carbon/carbon nozzle tests demonstrated that a better sealing system than the previously used dual layer, staggered finger seal was required. The finger seal was successful in keeping the exhaust products from escaping forward but was not able to prevent leakage of the gearbox dump flow used to pressurize the seal cavity (Ref. 1). The PIP test experience also demonstrated that it was desirable to continue to inject the gearbox dump flow into the area between the primary and secondary nozzles. This flow has a cooling effect in the boundary layer downstream of the joint. The flow is also theorized to have a stabilizing effect in the aerodynamic transition of the boundary layer between the two nozzles.

Another important finding from the PIP testing was that both of the seals, used to form a pressurized cavity between the nozzles, were not required. Testing showed that safe operation was achievable by placing a single seal in the upstream end of the cavity and leaving the downstream end open to the nozzle exhaust.

A number of seal schemes were evaluated before the lip seal shown in Figure 8 was selected. This seal is a metal reinforced graphite impregnated Teflon seal fabricated by Fluorocarbon Mechanical Seal Division in Los Angeles, California. The seal has been designed to maintain a contact pressure on each land of 0.5 to 10 lb/inch of circumference throughout the worst combination of thermal and mechanical tolerances in the nozzle. This has been achieved while still providing a maximum drag force, during nozzle deployment, of 90 pounds.
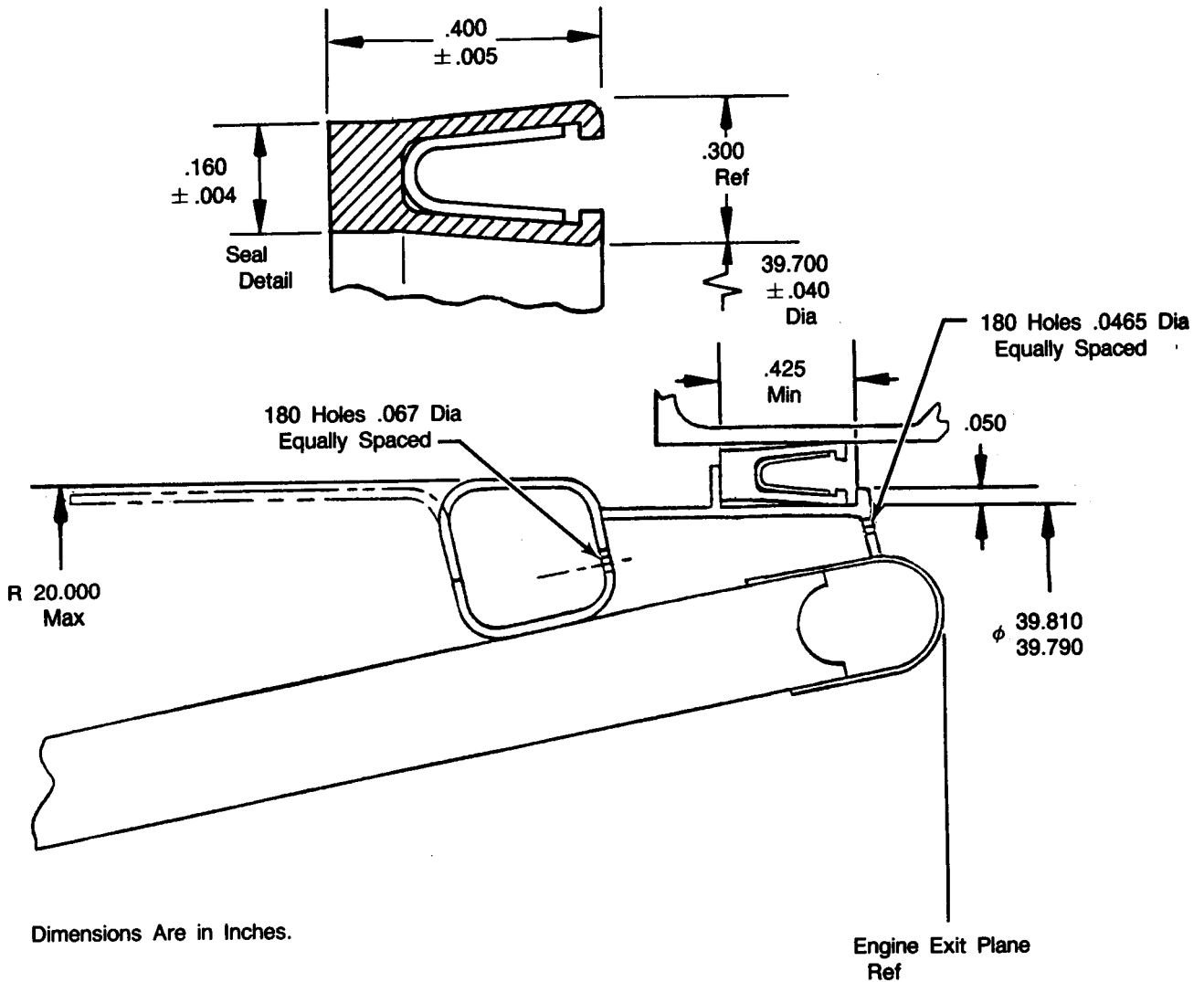
11

Figure 8. Flight Weight Nozzle Lip Seal

The seal gland or internal diameter support for the seal serves a dual purpose as a manifold for the gearbox dump flow into the seal cavity. The gearbox dump flow is routed into a cavity formed by capping the aft-most thrust chamber reinforcing band. From this cavity the gaseous hydrogen flows into a second cavity, from which it exits through 180 orifices equally spaced around the circumference of the nozzle, into the area between the two nozzles.

3097C

SECTION IV
STRUCTURAL ANALYSIS

A. SUMMARY

This structural analysis evaluates the 20-inch flight weight extendible nozzle made from C-103 columbium material. A previous columbium nozzle, Figure 9, was designed and analyzed but a redesign was required due to its high cost as well as new information on loading. This information was provided by the failure of a carbon/carbon 20-inch extendible nozzle, during shutdown on the test stand which led to a characterization of the shutdown pressure loading. This loading turned out to be much more severe than originally thought and governed the redesign effort. The redesigned columbium nozzle, Figure 10, was substantially stiffened by means of a removable ring to allow it to withstand shutdown pressure loading. Predicted shutdown stresses and deflections are acceptable; all other loading conditions, both ground and flight, are insignificant in comparison. Vibration due to acoustics may be a concern and should be monitored during testing.
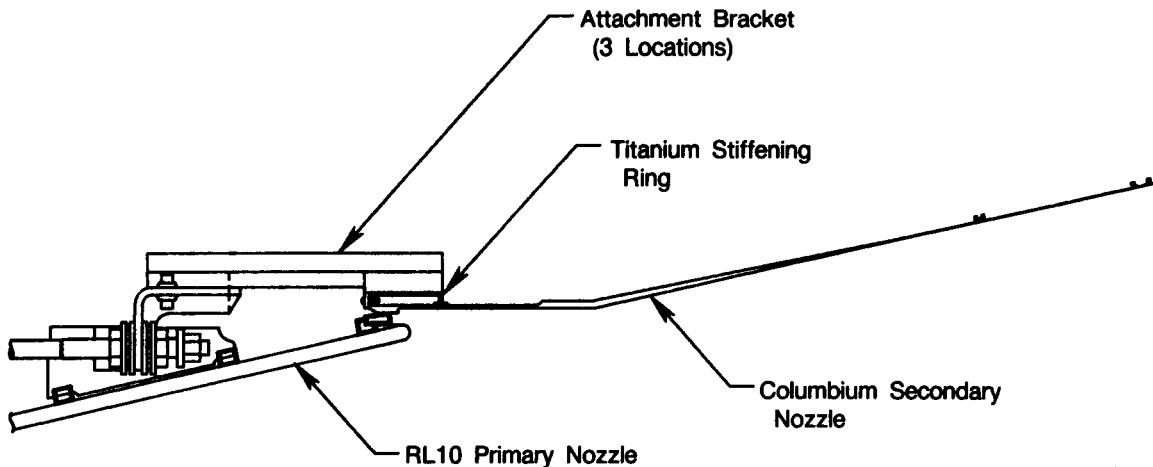
FD 329872

Figure 9. Original Columbium Nozzle Design

13

Removable Aluminum
Stiffening Ring (6061-T6)
(For Test Stand Only)

4.0 in.

44.0 in. Dia

7.0 in.

0.190 in.

0.100 in.

Columbium Secondary Nozzle
(C-103, PWA 1095)

Titanium Attachment Ring
(6-4 Ti, AMS 4928)

Attachment Latches
(12 Locations)
(6-4 Ti)

RLIO Primary Nozzle
(347 Stainless)
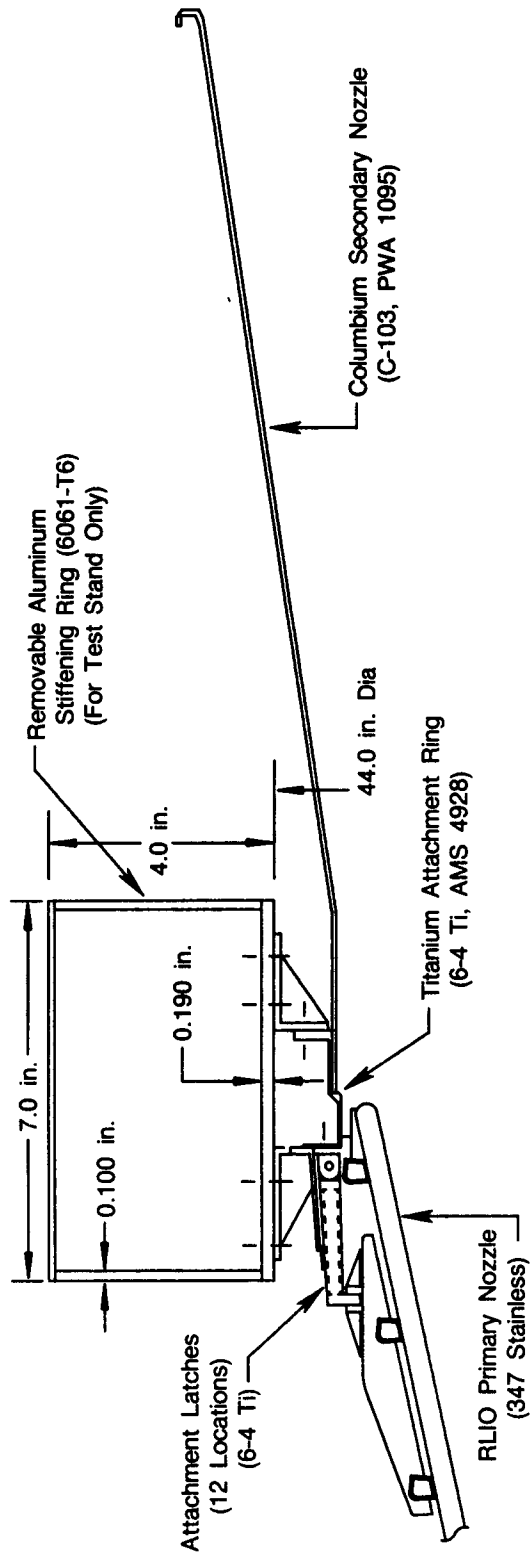
FD 329867

Figure 10. *Redesigned Columbium Nozzle*

14

B. INTRODUCTION AND BACKGROUND

An extendible nozzle such as the one shown in Section I, Figures 1 and 2 permits an increase in specific impulse by increasing the nozzle area ratio. This is accomplished without increasing overall launch vehicle length thus allowing a longer payload to be carried for the same launch length.

The 20-inch columbium flight weight nozzle was part of a NASA proof-of-concept design effort. This also included a 20-inch carbon/carbon "boiler-plate" nozzle that was built and tested. The design of the original columbium nozzle shown in Figure 9 had been completed when one of the carbon/carbon nozzles failed at shutdown in the test stand.

Subsequent investigation of the shutdown pressure environment showed a short duration, non-repeating, non-uniform pressure differential across the nozzle. This loading, which was much more severe than initially assumed, is caused by unstart of the test stand diffuser and by flow separation within the nozzle as chamber pressure and flow rate are reduced. It should be emphasized that this condition will only occur in the test stand and not in space.

Because of this new shutdown loading, as well as new data on the thermal loading, and because the complexity of the columbium portion of the original nozzle was driving up manufacturing costs, the nozzle was redesigned as shown in Figure 10. The basic approach to handling the shutdown loads was to stiffen the secondary nozzle where it attaches to the primary nozzle, mainly by means of a large removable stiffening ring, but also by tying the secondary nozzle to the relatively stiff primary nozzle at 12 locations rather than the original three. This approach allows the short, thin, large diameter secondary nozzle to behave as if it were part of a complete cone which is relatively stiff, rather than as a short, thin, large diameter unsupported cylinder which is relatively flexible, as was the case with the original design. The columbium portion of the nozzle was simplified to reduce cost by minimizing the amount of machining, welding and forming required and by substituting titanium for columbium where temperatures permitted.

C. LOADING

1. Test Stand Pressures

The test stand pressure loading was considered in the initial design, but it had been based on earlier data from a single pressure probe which measured a maximum pressure differential of 4.0 psi across the nozzle. It had been assumed that this 4.0 psi loading was uniform around the circumference. After the carbon/carbon nozzle failure, six pressure probes equally spaced around the exit plane of the secondary nozzle were installed. In subsequent carbon/carbon nozzle tests, these measured a highly non-uniform pressure distribution which lasts for about 0.1 second during shutdown. Figure 11 shows the time response of the pressure probes for a typical shutdown. The circumferential distribution of the peak pressures for this shutdown as well as seven others are shown in Figure 12. There appears to be no repeatable pattern. Because the loading is random it was treated statistically to yield a 3-sigma worst load distribution shown in Figure 13. This was arrived at by adding the 3-sigma worst probe-to-probe variation to the 3-sigma worst "circumferentially-averaged" pressure.

15

• Transient History for a Typical Engine Shutdown
• Data from Six Pressure Probes at Nozzle Exit Plane
• Only Occurs on the Test Stand

Nozzle ΔP-psi

Time from Shutdown Signal - sec
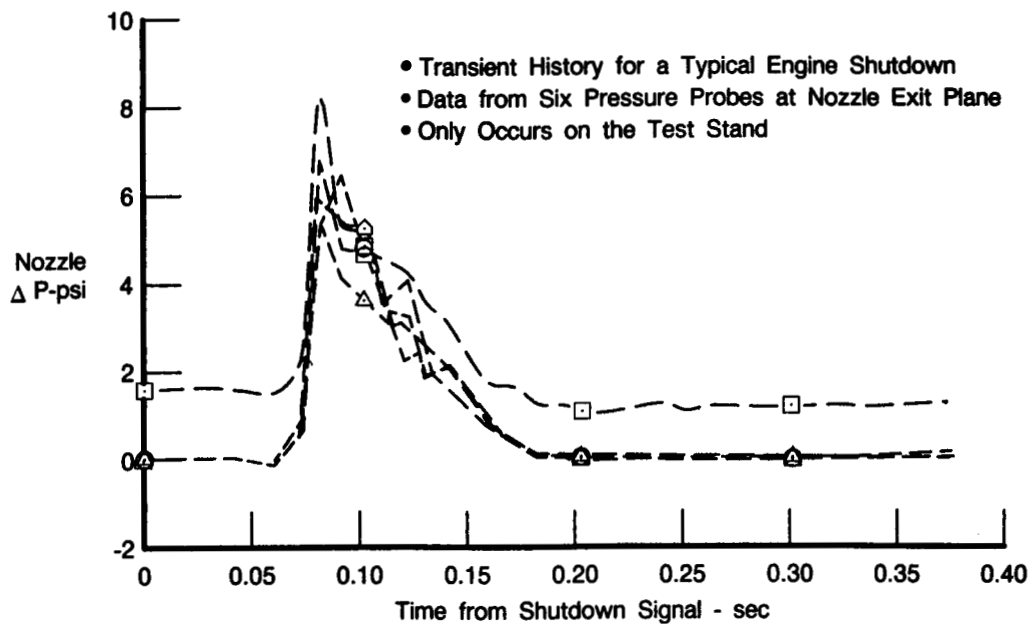
FDA 329874

Figure 11. Test Stand Shutdown Pressure Spike Data

• Circumferential Pressure Distribution at Time of max ΔP for Eight Engine Shutdowns
• Distribution is Non-Axisymmetric and Non-Repeatable

Nozzle ΔP (psi)

Pressure Probe No.

Circumferential Location - degrees
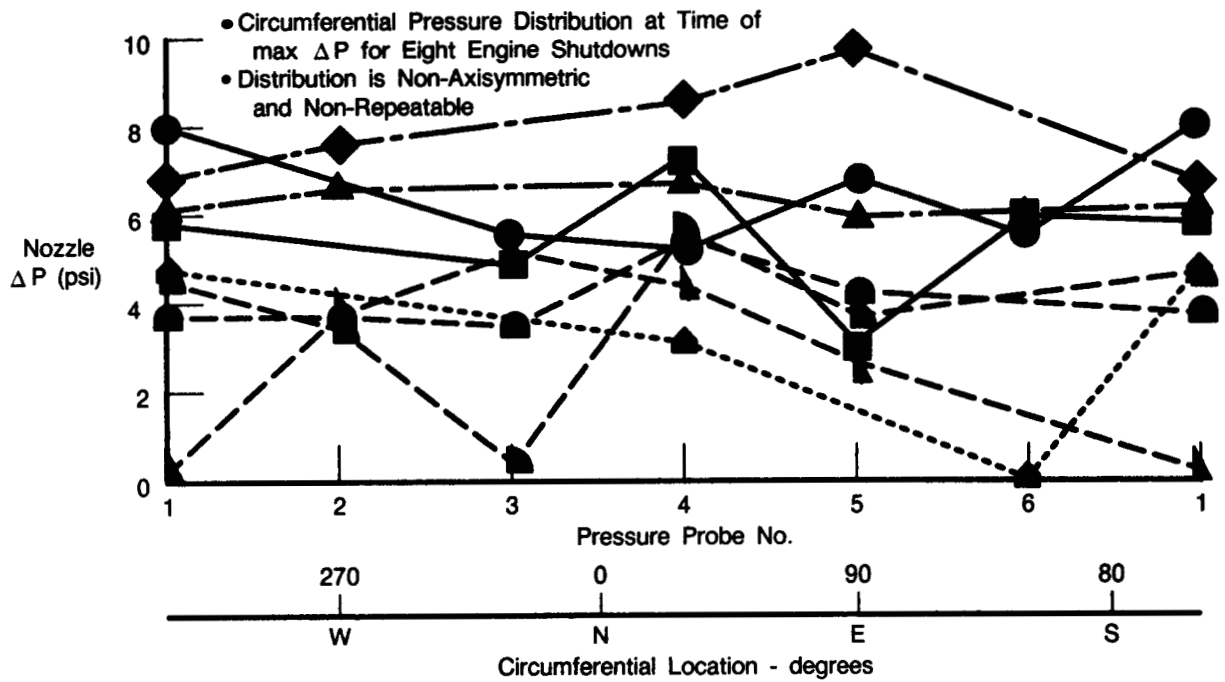
FDA 329875

Figure 12. Circumferential Pressure Distribution at Time of Maximum ΔP for Engine Shutdowns
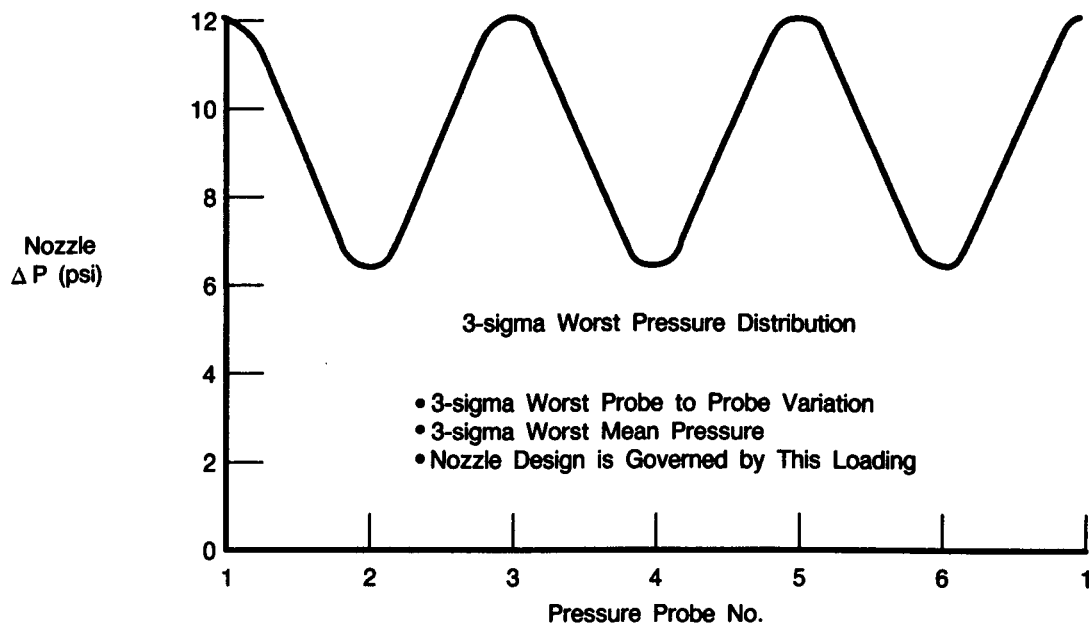
16

Figure 13. Idealized 3-Sigma Worst Case Test Stand Shutdown Pressure Loading

The idealized 3-harmonic sinusoidal variation was chosen for ease of modeling in the stress analysis, however, comparison of Figures 12 and 13 showed none of the data to have a 3-harmonic characteristic. This turned out to be irrelevant as the stress analysis showed that the important driver on stress was not the number of minimum to maximum pressure variations per se, but rather the span over which they act. Maximum stresses for a ½ cycle pressure variation from 6 to 12 psi over 60 degrees of circumference is almost as bad as three full cycles over 360 degrees. As shown in Figure 12 most of the pressure distributions have their minimum and maximum pressures occurring between two adjacent probes, i.e., 60 degrees.

The shutdown loading is characterized by a short duration pressure spike which can reach peak ΔP in 10 msec. This is a dynamic loading which would usually require that a load factor of 1.5 to 2.0 be applied to the measured pressure distribution to take into account inertial loads and their resulting increase in stress. This increase is due to the rapid loading which causes rapid deflection and momentum buildup in the structure. This must be stopped by additional straining of the material over and above the pressure induced strain.

There was no dynamic load factor applied to the 3-sigma worst case shutdown pressures. This is rationalized by the following arguments: 1) to design to such a loading would require making the nozzle prohibitively heavy; 2) the loading has already been made severe by choosing the 3-sigma worst case pressures; and 3) dynamic loading on most material results in significant viscous effects which increase the stiffness and yield; this means that while the dynamic loading may increase stress it also increases material capability.

2. Thermals

New temperature predictions (Ref. 1 and 2) were made after the initial design. These were based on data from testing of the carbon/carbon nozzle and are discussed in more detail in Section V. The same set of temperatures is used for both test stand and flight conditions. The effect on temperatures from the slight change in radiation cooling in the test stand is negligible.

17

3. Flight Pressure

Flight pressures vary in the axial direction from 1.0 psi ΔP at the primary nozzle exit plane to 0.6 psi ΔP at the secondary nozzle exit plane. In the circumferential direction the loading is uniform. For simplicity and conservatism in the stress analysis, a 1.0 psi uniform internal pressure was used.

4. Maneuver Loads

Maneuver loads are due to gimbaling of the RL10 engine and result in inertial loads on the secondary nozzle. The maximum gimbaling accelerations (from Ref. 3) are 38 rad/sec^2 simultaneously in both pitch and yaw. These can occur while the engine is firing.

5. Vibrations

The engine specification (Ref. 3) requires the engine to withstand any self-induced vibrations such as from pump or turbine rotors or from acoustic sources. In addition, a mechanical vibratory environment is specified which the nozzle must withstand. However, this environment is caused by launch forces which occur when the nozzle is in the stowed position in the launch vehicle. Since the stowed latching system was not designed for this demonstration program, this specified vibratory environment was not considered. It is envisioned that this situation would be easily handled by providing expendable supports for the nozzle in its stowed position. One potential approach is to place foam inserts between the thrust chamber and the nozzle extension at the nozzle exit plane. These inserts would support the nozzle during the boost phase and would be ejected during nozzle deployment.

D. STRESS ANALYSIS

1. Original Analysis Method

NASTRAN was used to analyze the original columbium nozzle. It was chosen because of the 3-D nature of the original geometry caused by the three-point support system. While the primary or secondary nozzles could be analyzed separately with axisymmetric models, joining them together at three discrete locations required a large NASTRAN plate element model existing in 3-D space.

2. Redesign Analyses Method

For the redesigned nozzle an axisymmetric shell analysis was used (Shell deck, W526). This was chosen because the number of supports or latches was large enough, 25 initially, to approximate an axisymmetric tie between the primary and secondary nozzles using modified or reduced properties in the latch region. It was also chosen because the shell analysis was less costly and faster to run than NASTRAN for the many iterations required.

As the redesign effort progressed, the number of latches was reduced to 12 causing concern that the assumption of axisymmetric boundary conditions might no longer be valid. As a result, a study was conducted comparing results from a NASTRAN model with discrete latches and the shell deck as a function of the number of latches. This is presented in Appendix A and shows good agreement between NASTRAN and shell deck stress results.

3. Shell Model

The redesigned columbium nozzle shell model is shown in Figure 14. It includes the aluminum box stiffening ring and the primary nozzle from the exit plane to the coolant manifold (a radial hardpoint).

18

Removable Stiffening Ring

Redesigned 20" Columbium
Secondary Nozzle

Primary Nozzle

Coolant Manifold
(Same Hoop Stiffness)
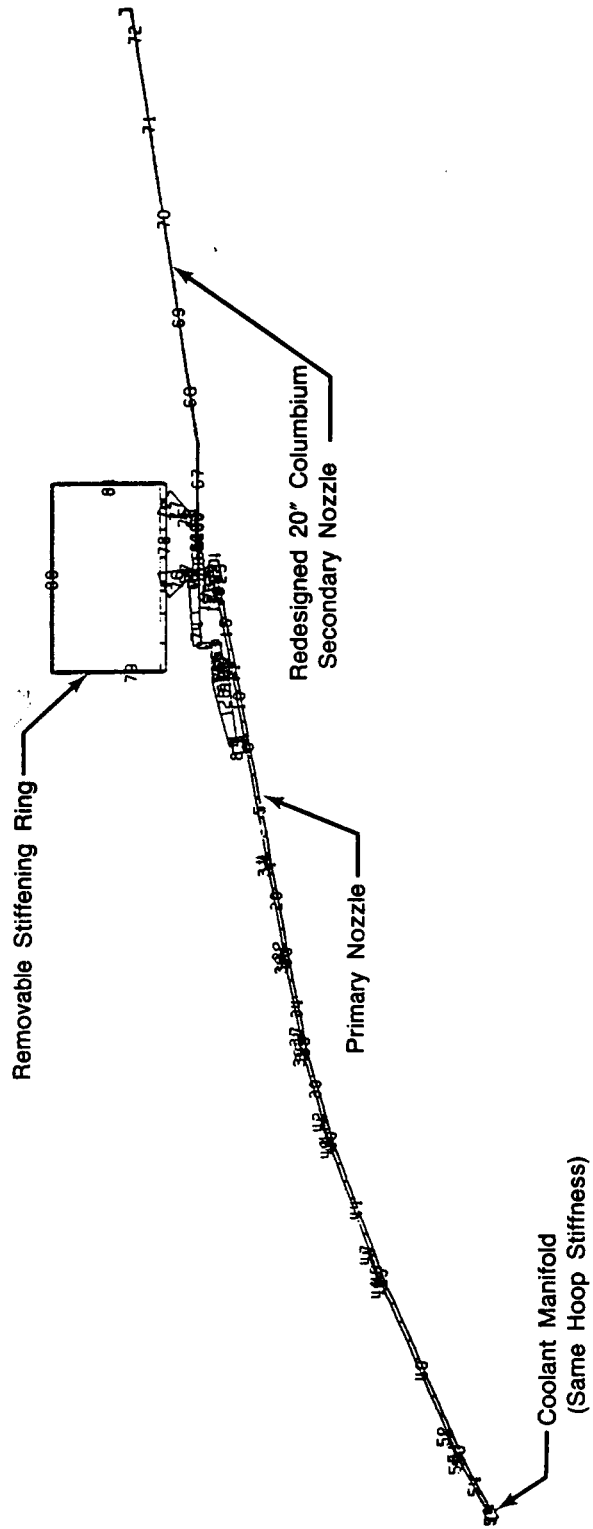
FD 329677

Figure 14. Flight Weight 20-inch Cb Nozzle Shell Model

19

E. TEST STAND SHUTDOWN PRESSURE STRESSES

1. Original Nozzle

A rough cut shell analysis of the original columbium nozzle geometry with approximated support stiffness was made for the new shutdown pressure loading to get a ballpark assessment of the stresses. The results, shown in Figure 15, predict gross deformations and failure of the nozzle. This is not surprising in light of the failure of the much stiffer carbon/carbon nozzle and is due to the softness of the support system. The original columbium nozzle in-flight configuration was attached to the primary nozzle through three latches which acted only in one direction to take out thrust loads. It was supported in the other direction by three guide rod link arm bumper springs which provided minimal restraint of rearward axial deflection. This is essentially a spring-mounted axially "soft" support system which allows the harmonic component of the shutdown pressure to impose large radially outward and inward deflections. These are coupled to large axial fore and aft deflections as well as large circumferential deflections creating high nozzle strains. Stiffening the supports reduces these deflections and was the approach taken for the redesigned nozzle.

2. Redesigned Nozzle

The redesigned nozzle initially used 25 latches to tie into the relatively stiff primary nozzle which was assumed to act as a rigid ground for simplicity in the shell analysis. This approach reduced stresses and deflections to acceptable levels as shown in Figure 16 but created large latch loads required to resist the harmonic component of the pressure load.

There was concern that these high latch loads would cause problems for the primary nozzle. If these loads could cause significant deflections of the primary nozzle, then the results in Figure 16, which assumed a rigid primary nozzle, would be invalid. This turned out to be the case when a shell analysis of the secondary nozzle joined to the primary resulted in unacceptable stress levels in both (Figure 17).

To absorb the load and reduce stresses, additional structure was required. Since this would only be needed for test stand loading, a removable stiffening ring was designed which would only be used for ground testing and not for flight. Adding this ring to the shell model produced acceptable stresses as shown in Figure 18. However, pressure loading is only part of the total loading; thermal loading was also considered.

20

Predicting Gross Deformations and Failure

$\sigma_{von\ Mises} = 819$ ksi
$\delta_{AXIAL} = 11.1$ in.
$\delta_{RADIAL} = 29.0$ in.
$\delta_{CIRC} = 9.2$ in.
(at 30°)

Leaf Spring
(Representing Guide Rod
Bumper Spring Rate)

$\sigma_{von\ Mises} = 97$ ksi
$\delta_{AXIAL} = -8.2$ in.
$\delta_{RADIAL} = 1.1$ in.
$\delta_{CIRC} = -0.4$ in.
(at 30°)

$\sigma_{von\ Mises} = 101$ ksi

Leaf Spring
(Representing the Teflon
Seal Radial Springrate)
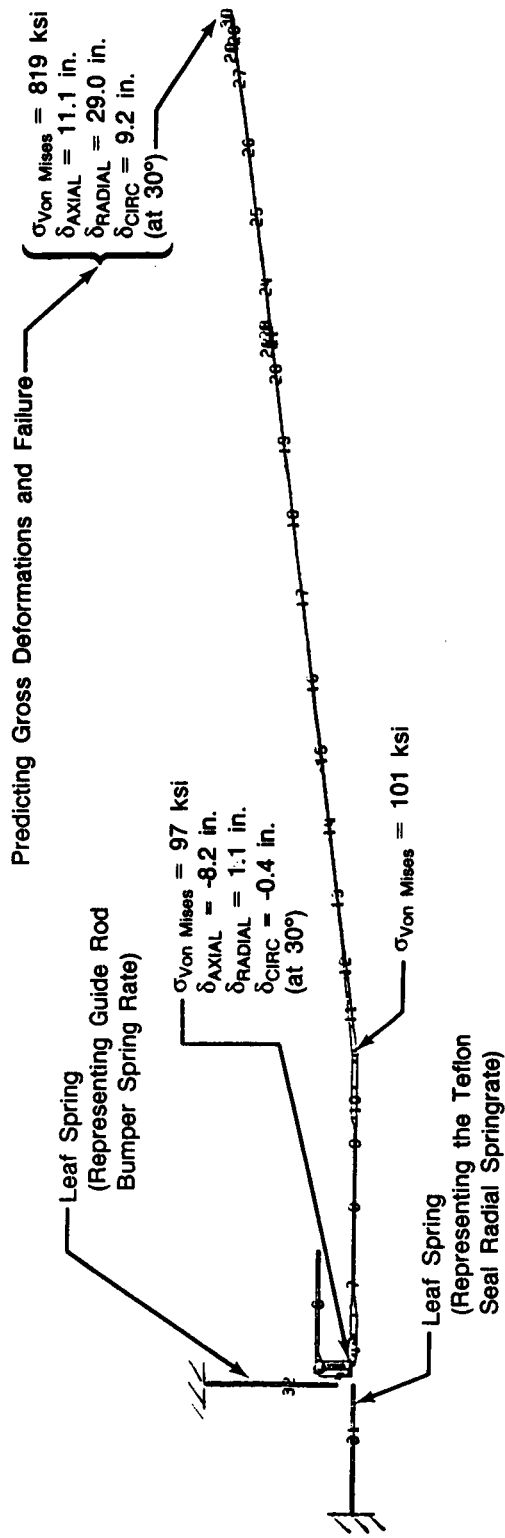
FD 329914

Figure 15.   Original Cb Secondary Nozzle Shell Model Test Stand Shutdown Stresses and Deflections (at 0°-Point at Which Max Pressure Occurs — 12.1 psi)

21

$P_{RADIAL} = 73$ lb/in.
$P_{AXIAL} = 375$ lb/in.
$P_{CIRC} = 251$ lb/in.
(at 30°)

$\sigma_{Von\ Mises} = 53$ ksi
$\sigma_{YIELD} = 111$ ksi
$\delta_{RADIAL} = 0.04$ in.
$\delta_{AXIAL} = -0.03$ in.

$\sigma_{Von\ Mises} = 23$ ksi
$\sigma_{YIELD} = 32$ ksi

$\sigma_{Von\ Mises} = 8$ ksi
$\sigma_{YIELD} = 24$ ksi
$\delta_{RADIAL} = 0.24$ in.
$\delta_{AXIAL} = -0.07$ in.

Latches

Unconservative Boundary Conditions
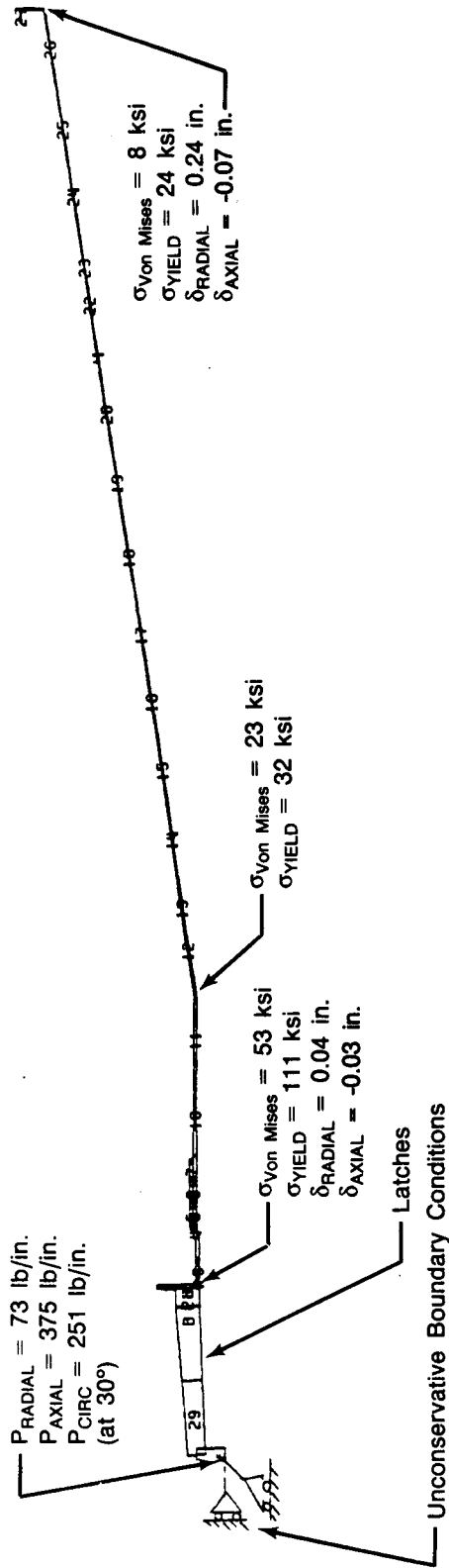
FD 329915

Figure 16. Flight Weight 20-inch Cb Nozzle Shell Model — Early Configuration — Test Stand Shutdown Stresses Deflections and Loads (at 0°)

22

$\sigma_{von\ Mises}$ = 90 ksi
σ_{YIELD} = 24 ksi
δ_{RADIAL} = 1.60 in.

$\sigma_{von\ Mises}$ = 162 ksi
σ_{YIELD} = 30 ksi
δ_{RADIAL} = 0.63 in.

P_{RADIAL} = 90 lb/in.
P_{AXIAL} = 342 lb/in.
P_{CIRC} = 253 lb/in.
(at 30°)

σ_{VM} = 112 ksi
σ_{YIELD} = 30 ksi

P_{AXIAL} = 570 lb/in.
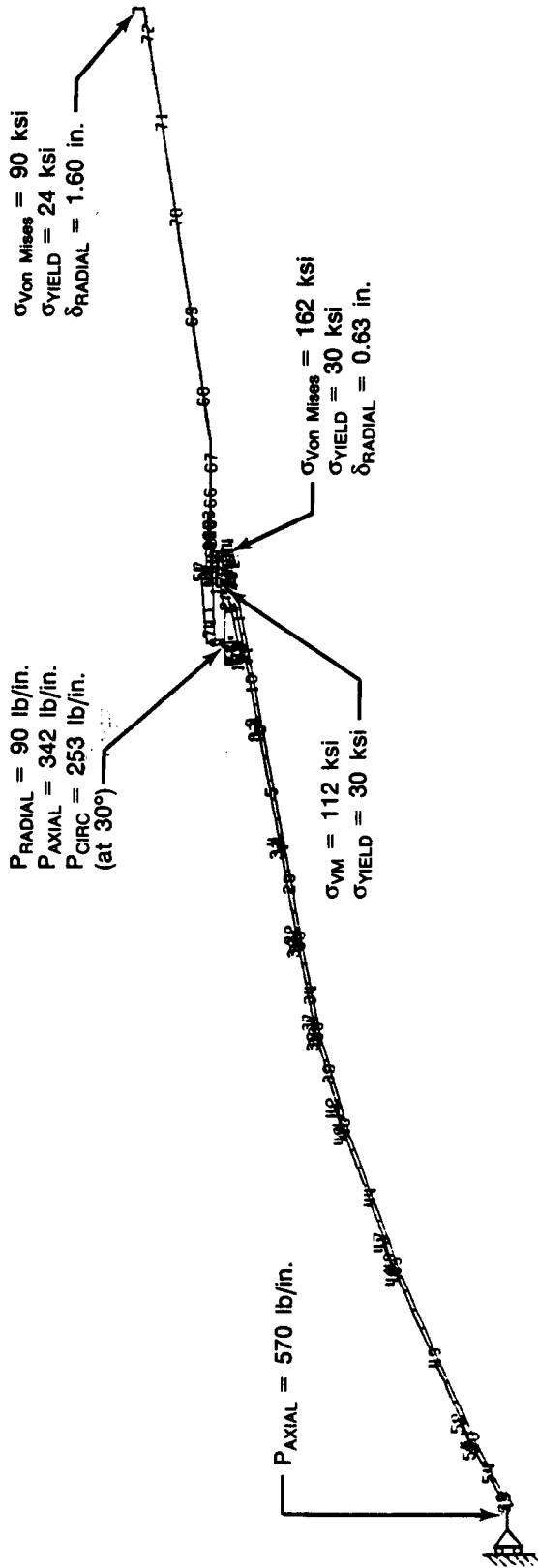
FD 329916

Figure 17. Combined Primary-Secondary Nozzle Shell Model Test Stand Shutdown Loading Stresses and Deflections (at 0°)

23

3097C

(Includes Ground Test Ring)

σ_{VM} = 48 ksi
σ_{YS} = 125 ksi

σ_{VM} = 15 ksi
σ_{YS} = 23 ksi

σ_{VM} = 21 ksi
σ_{YS} = 24 ksi

σ_{VM} = 13 ksi
σ_{YS} = 24 ksi
δ_{RAD} = 0.20 in.

σ_{VM} = 23 ksi
σ_{YS} = 28 ksi
P_{RAD} = 17 lb/in.
P_{AX} = 209 lb/in.
P_{CIRC} = 116 lb/in.
(at 30°)

P_{RAD} = 33 lb/in.
P_{AX} = 130 lb in.
P_{CIRC} = 5 lb/in.
(at 30°)

σ_{VM} = 14 ksi
σ_{YS} = 30 ksi

σ_{VM} = 10 ksi
σ_{YS} = 30 ksi
δ_{RAD} = 0.024 in.

FD 329917

Figure 18. Final Configuration (Test Stand) — Shell Model Test Stand — Shutdown Pressure Loading Only — Stresses, Deflections and Loads (at 0°)

24

3. Thermal Stresses

The temperatures were input to the shell model without pressure loading (harmonic pressures and uniform temperatures cannot be run at the same time in the shell deck). The stresses for this loading are listed in Figure 19. These stresses are low due to the relatively low temperature levels and gradients and because of the low coefficient of thermal expansion of columbium.

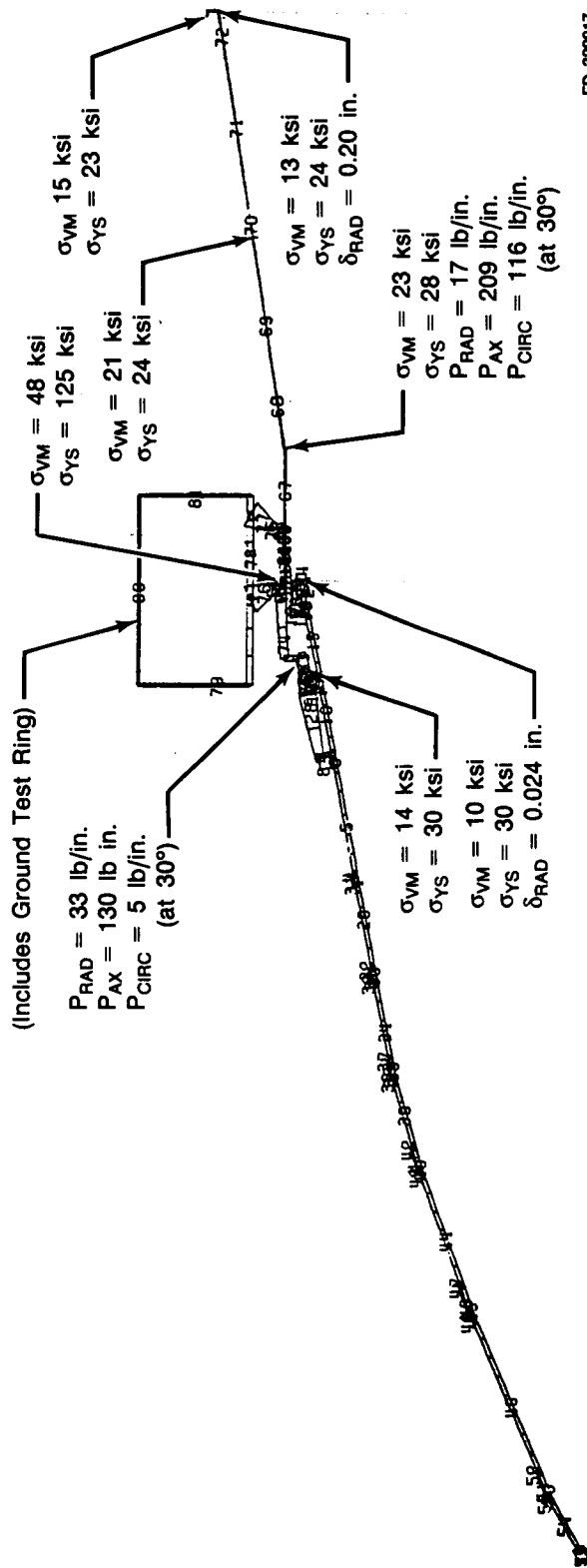## 4. Test Stand — Combined Stresses

The pressure load stresses and thermal stresses were combined to yield total stresses as shown in Figure 20. Stresses are less than yield everywhere except at the throat region where they are slightly over yield. This means that if the nozzle experiences the 3-sigma worst case pressure loading then some level of permanent deformation will occur in the vicinity of the throat. This should not affect nozzle function.

5. Flight Stresses

The flight stresses shown in Figure 21 are little more than the thermal stresses with a small increase due to the 1.0 psi uniform internal pressure. The flight loading is almost insignificant in comparison to the test stand loading.

$\sigma_{vm} = 8 \text{ ksi}$

$\sigma_{vm} = 0 \text{ ksi}$

$\sigma_{vm} = 4 \text{ ksi}$

$\delta_{RAD} = 0.093 \text{ in.}$

$\sigma_{vm} = 10 \text{ ksi}$

$\sigma_{vm} = 10 \text{ ksi}$
$\sigma_{ys} = 125 \text{ ksi}$

FD 329918

Figure 19. Final Configuration (Test Stand) — Shell Model — Thermal Loading Only — Stresses and Deflections

26
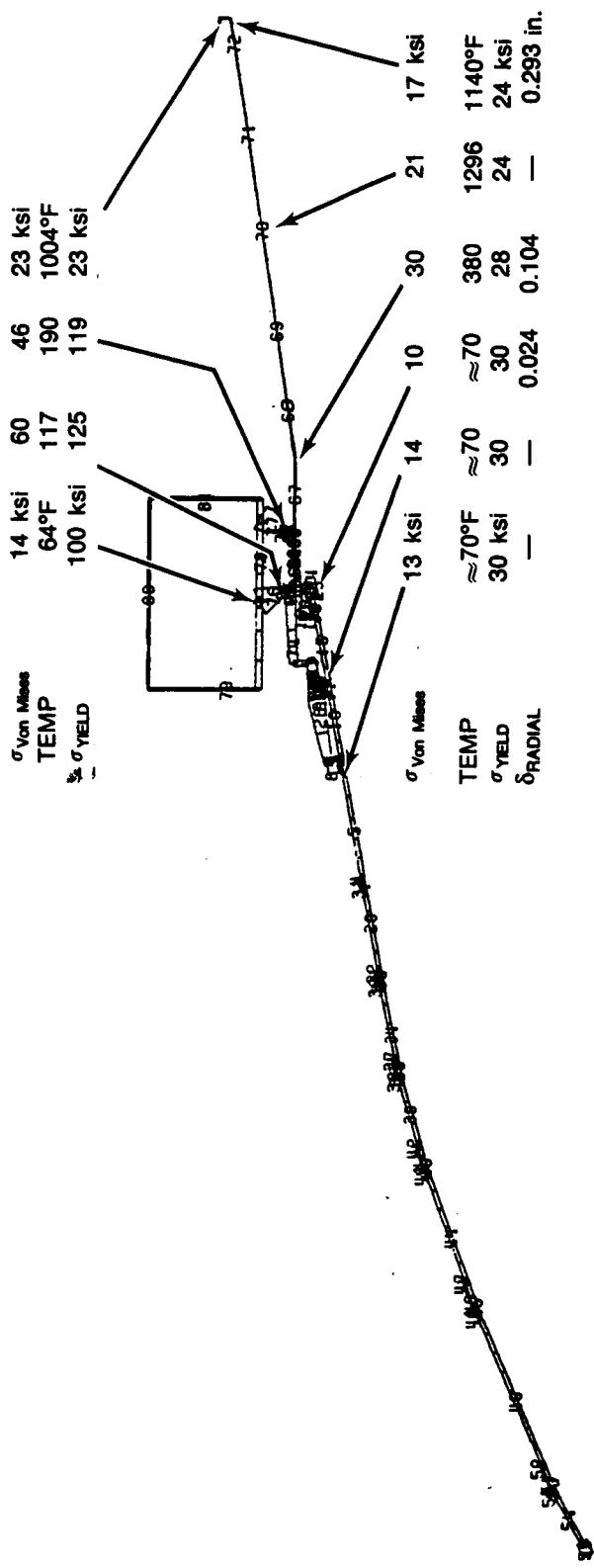
Figure 20. *Final Configuration (Test Stand) — Shell Model Test Stand Loading — Pressure and Thermal Stresses and Deflections (at 0°)*

27

Figure 21. *Final Configuration (Flight) — Shell Model Analysis — Flight Loading — Pressure and Thermal Stresses (Von Mises Stress) — Ring Removed*
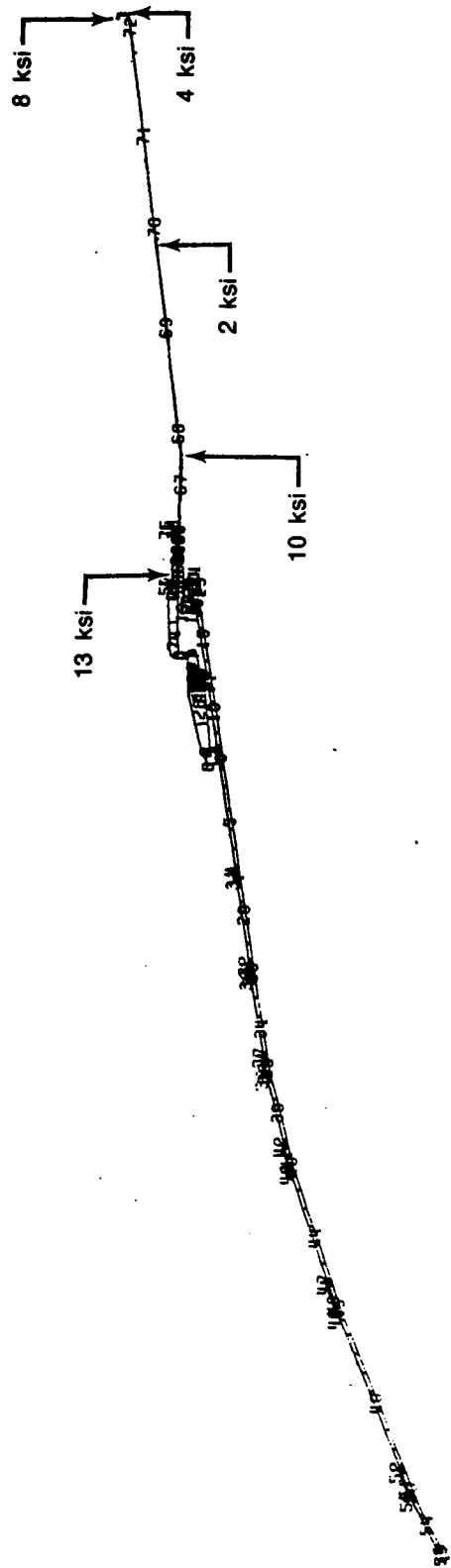
FD 329920

28

6. Maneuver Stresses

Maneuvers or g-loading effects were approximated using the shell deck. The required 38 rad/sec^2 yaw and pitch accelerations were vector summed to a single 54 rad/sec^2 acceleration. This was then applied to the secondary nozzle mass which was conservatively assumed to act at the exit plane. Normal and tangential components of force were then calculated and applied as a distributed axial and lateral load acting at the exit plane circumference of the shell model as shown in Figure 22. This is conservative since the actual inertial load is distributed over the entire secondary nozzle area. Figure 22 also lists stresses; as shown, they are low and, even if combined with the flight loading, produce no stresses over yield. This analysis did not consider the maneuver loads on the entire nozzle structure because it would have required a large NASTRAN analysis and was outside the scope of this effort. However, the approximate maneuver stresses in Figure 22 show that the secondary nozzle causes relatively small levels of additional stress to be added to the primary nozzle structures.
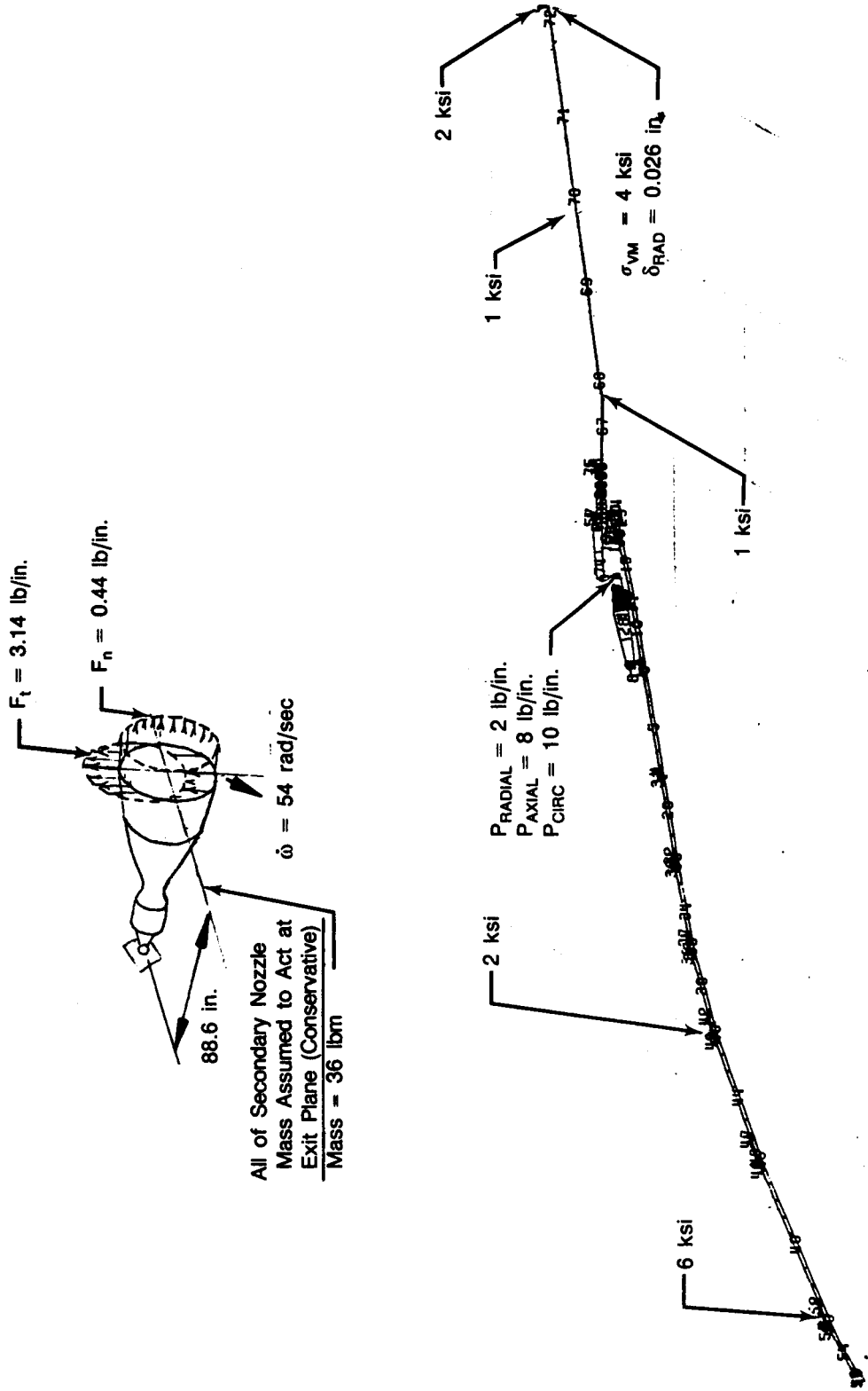
7. Vibration

Natural frequency analyses were made for both the test stand and flight configurations. The fundamental frequencies and mode shapes are shown in Figures 23 and 24. Potential drivers of these modes are mechanical excitation from pump and turbine rotor unbalance and acoustic excitation from flow turbulence.

Based on the Campbell plot in Figure 25 there should be no mechanically induced resonance since the natural frequency of the nozzle is well above the LOX pump excitation frequency and well below the fuel pump excitation frequency.
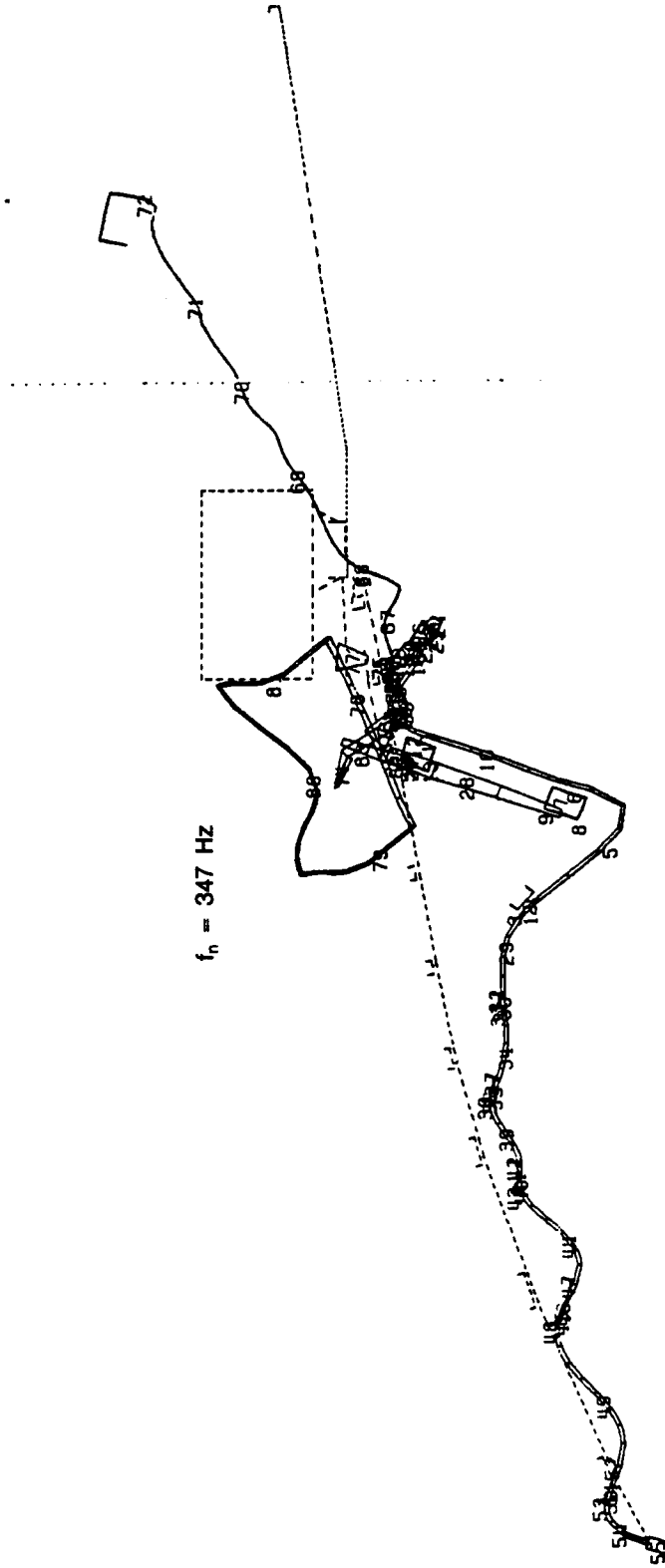
Acoustic vibratory loads may be a problem since there can be a major source of acoustic energy provided by the turbulence in the step or "waterfalls" between the primary and secondary nozzles. The potential of this energy source was demonstrated by earlier testing of the carbon/carbon nozzle which shook when hydrogen, from the gearbox dump, introduced at the step, was shut off. The gearbox dump flow probably smooths the boundary layer between the two nozzles reducing the turbulence and thus the acoustic energy. The purge system on this redesigned columbium nozzle introduces the H$_2$ gas at a different radial location than in the carbon/carbon nozzle system; this may or may not be as effective in reducing turbulence. It is impossible to predict whether acoustic loading will be a problem before the engine runs since the acoustic environment is not known beforehand. Because of the unknowns involved, it is recommended that accelerometers and kistlers or kulites be placed on the cooler portions of the secondary nozzle so that if a problem does occur there will be enough information available to identify the source, to quantify it, and work toward a fix.

The RL10 engine specification (Ref. 3) requires the engine to withstand an externally imposed vibratory environment. This loading would be caused by vehicle launch loads when the secondary nozzle is in the stowed position. The stowed mounting and latching system provides the boundary conditions of the stowed secondary nozzle, and since this was not designed as part of this effort, the external vibratory loading could not be considered.

$F_t = 3.14$ lb/in.

$F_n = 0.44$ lb/in.

88.6 in.

All of Secondary Nozzle
Mass Assumed to Act at
Exit Plane (Conservative)
Mass = 36 lbm

$\dot{\omega} = 54$ rad/sec

$P_{RADIAL} = 2$ lb/in.
$P_{AXIAL} = 8$ lb/in.
$P_{CIRC} = 10$ lb/in.

2 ksi

1 ksi

2 ksi

1 ksi

$\sigma_{VM} = 4$ ksi
$\delta_{RAD} = 0.026$ in.

2 ksi

6 ksi

FD 329921

Figure 22. Maneuver Load Stresses — Simulated

30

3097C

$f_n = 347$ Hz

FD 329922

Figure 23. Fundamental Mode — Test Stand Configuration from Shell Deck Natural Frequency Analysis (1st Mode of 1st Harmonic)

31

$f_n = 367$ Hz
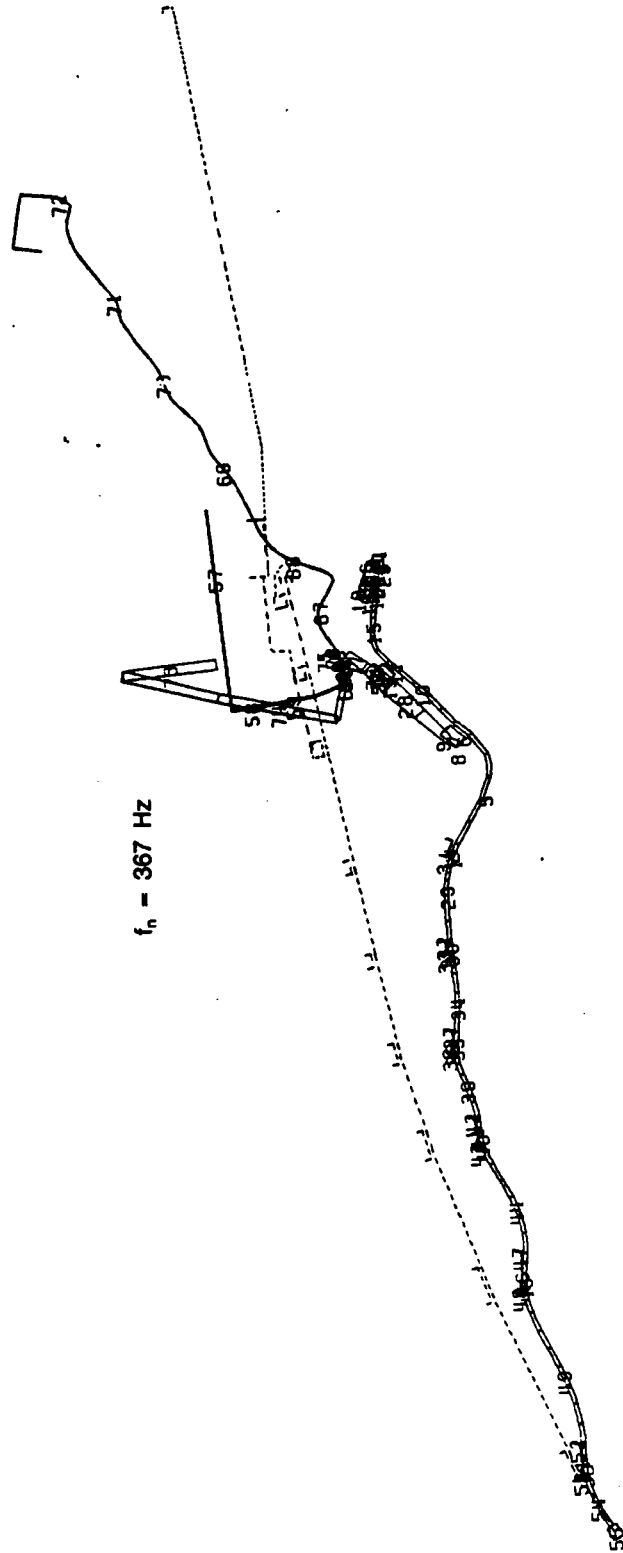
Figure 24.   Fundamental Mode — Flight Configuration from Shell Deck Natural Frequency Analysis (1st Mode of 1st Harmonic)

FD 329923

32
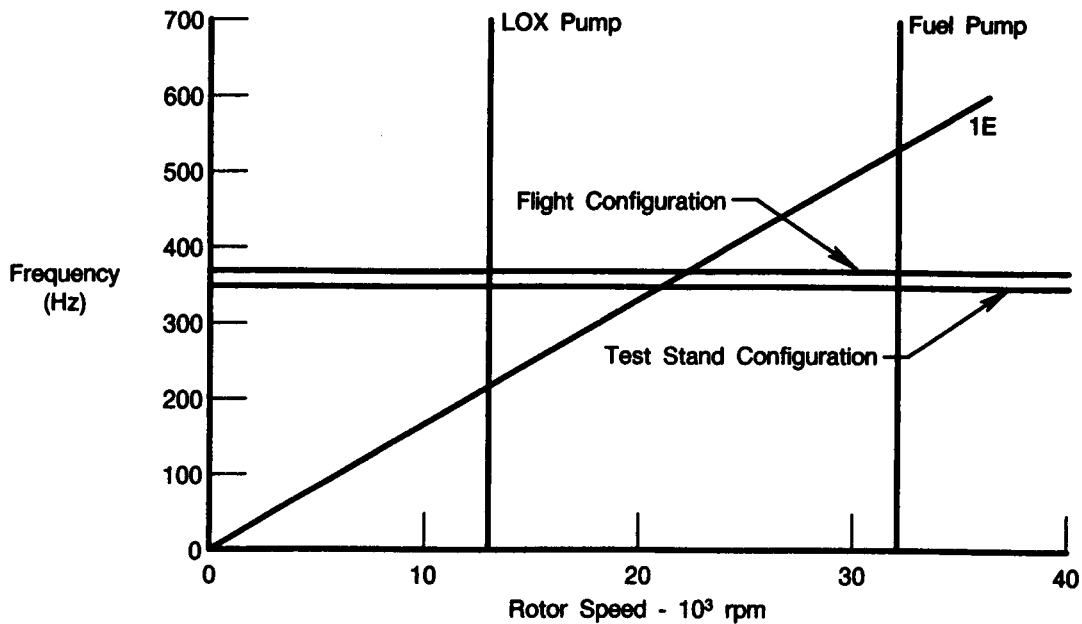
Figure 25. 20-Inch Cb Nozzle Campbell Diagram

8. Latch Hardware Stresses

The latches and associated hardware had initially been designed to handle the high latch loading for test stand shutdown as predicted in Figure 16. The latch loading for the final configuration with stiffening ring (Figure 18) is less, even with the reduced number of latches (12 vs 25). The worst latch load produced stresses for this configuration that were well below yield as shown in Figure 26.
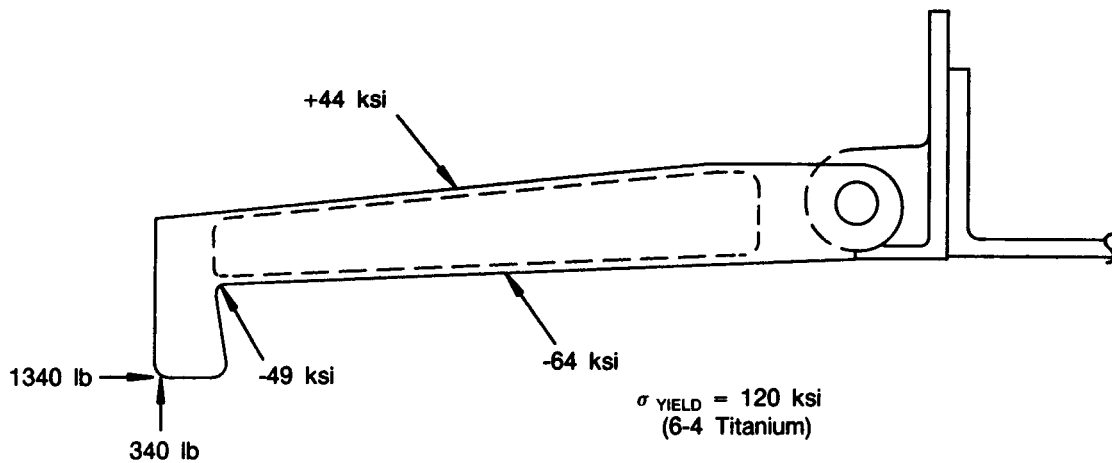
Figure 26. Latch Loads and Stresses for Test Stand Shutdown for the Most Highly Loaded Latches (at 0°, 60°, 120°, etc.)

F. HARMONIC LOADING SENSITIVITY STUDY

As part of the analysis of the test stand shutdown loads it was noticed that a 3-harmonic pressure loading produced larger stresses in the secondary nozzle than a 1-harmonic loading of the same amplitude. Therefore, a sensitivity study was made to qualitatively assess the effects of stress vs the number of harmonics for the redesigned columbium nozzle. Figure 27 shows the harmonic loading used and the resulting hoop bending stress for two cases: the final redesigned config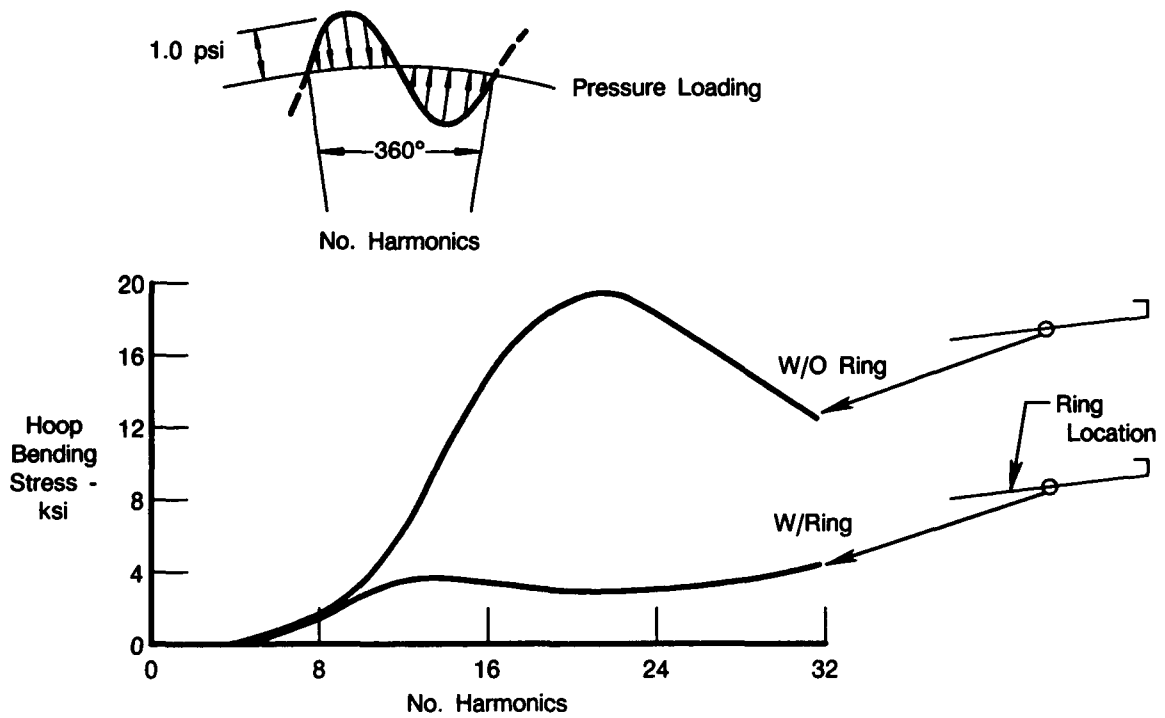uration with only the exit plane stiffening ring; and a modification with an additional mid-stiffening ring. As shown in Figure 27, the baseline nozzle is most sensitive to a 20 to 24-harmonic loading. Again, the important driver on stress is not the number of pressure variations per se but rather the span over which the minimum to maximum pressure acts. A 20 to 24-harmonic loading means a minimum to maximum pressure variation over a 3 to 4-inch span. The reason for this behavior is that as the harmonic number increases the nozzle is loaded less like a hoop, which has good in-plane stiffness, and more like a large span thin (0.015 in.) plate, which has poor bending stiffness. Eventually, as the harmonic number increases, the span of the loaded "plate" decreases causing the bending stiffness to increase.

Figure 27. *Harmonic Loading Sensitivity Study*

It is unknown if the test stand shutdown pressure loading has any harmonic components higher than three since only six pressure probes were used. But if they did exist they would tend to promote axial corrugations or "wrinkling" of the nozzle, which could cause loss of the brittle silicide coating on the columbium.

34

Experience with the Space Shuttle Orbital Maneuvering System (OMS) engine nozzle has demonstrated that this wrinkling can occur. The OMS engine nozzle is a columbium nozzle comparable in diameter to the RL10 secondary nozzle, but thicker. The loading on the OMS nozzle may be more severe since it experiences aerodynamic loading during ascent and reentry. While this loading may not be the same magnitude, it is the same type of unsteady aerodynamic loading that the RL10 nozzle will see at shutdown. If wrinkling does turn out to be a problem on the columbium nozzle, then as Figure 27 indicates, a mid-stiffening ring should solve it. Adding a ring at this time is not recommended.

G. MATERIAL PROPERTIES

The material properties for C-103 columbium and Ti-6Al-4V (AMS 4928) are presented in Figures 28 and 29.
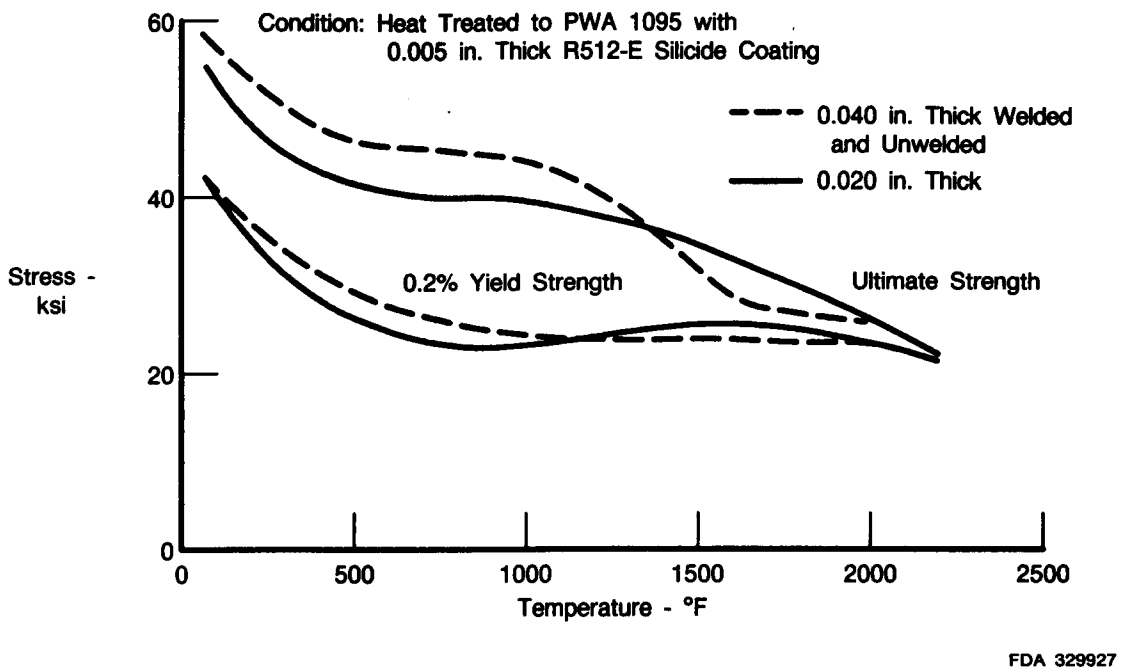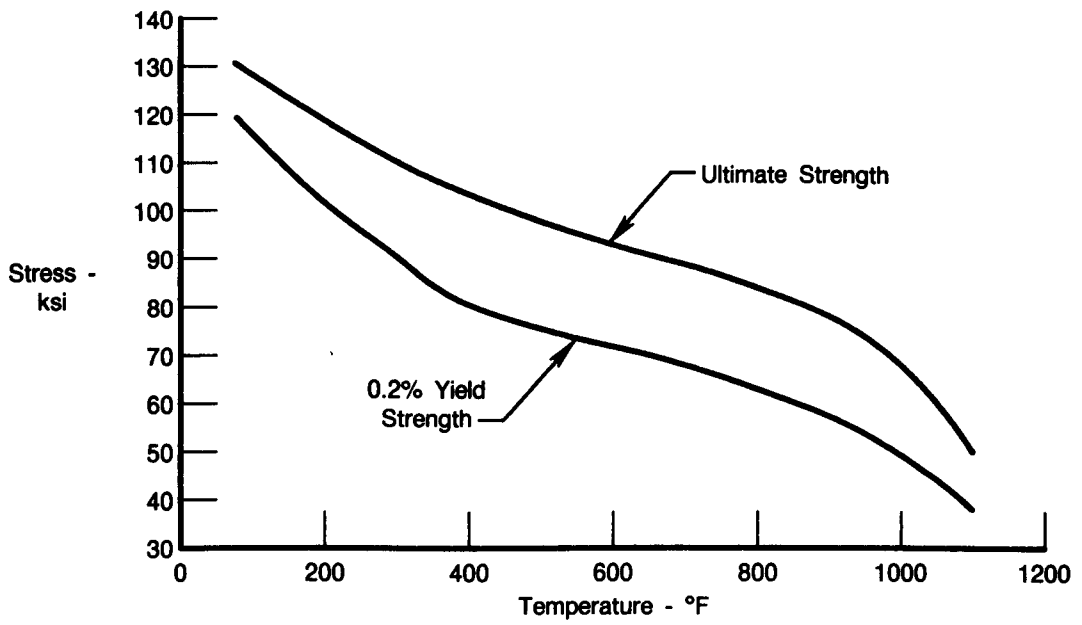

FDA 329927

Figure 28.   Material Strength Properties of Columbium C103 Used in the Analysis

35

Figure 29. Material Strength Properties of Titanium Ti-6Al-4V Used in the Analysis

FDA 329928

36

SECTION V
THERMAL ANALYSIS

The flightweight 20-inch Cb nozzle has been thermally designed as a radiation-cooled nozzle which also uses the benefits of the cooling effects from the water condensate and film cooling formed by the RL10 thrust chamber. This water condensate is formed when the steam produced by the RL10 combustion process is condensed, as it comes in contact with the low-temperature regeneratively-cooled thrust chamber walls. The water condensate from the thrust chamber wets the forward end of the nozzle and provides vapor film cooling to the rest of the nozzle. The effects of the water condensate have been verified by temperature measurements on the carbon/carbon (c/c) samples tested and video recordings which clearly show the water as it leaves the thrust chamber. In the video recordings, liquid water can be seen several inches downstream of the engine exit plane.

Additionally, over 2½ hours of c/c nozzle testing and the data obtained has allowed P&W to improve its rocket nozzle temperature prediction techniques* by incorporating the test results in the prediction methods. This testing had shown cooler than predicted nozzle temperatures, by approximately 300°R, in the 20-inch c/c nozzle.

The cooler wall temperatures have been determined to be caused by the cooling effect of the cool boundary layer on the primary nozzle. The cool boundary layer, in conjunction with the water condensate from the primary nozzle, provides a cooler film on the 20-inch nozzle than calculated in the original model. The film cooling temperatures were analytically determined by using Ref. 4 and the test data results.

The improved prediction techniques have been used to calculate the flight weight 20-inch Cb nozzle thermal environment used to design the nozzle. These temperatures are shown in Figure 30. This figure also shows the steady-state temperatures experienced in the nozzle seal area. These temperatures were calculated for the RL10A-3-3A engine conditions (O/F of 5.0:1 and 16.5K lb thrust). The maximum temperature in the Cb nozzle is 1774°R. It occurs 18 inches aft of the exit plane of the primary nozzle. For the RL10A-3-3B engine conditions (O/F of 6.0:1 and 15K lb thrust), the nozzle temperatures are expected to be approximately 60°R higher in the aft half of the nozzle while the temperatures in the forward half of the nozzle will be unchanged from those in the RL10A-3-3A case.

---

* An explanation of the methodology used to evaluate the RL10 nozzle thermal environment can be found in Section III-C of Ref. 1.
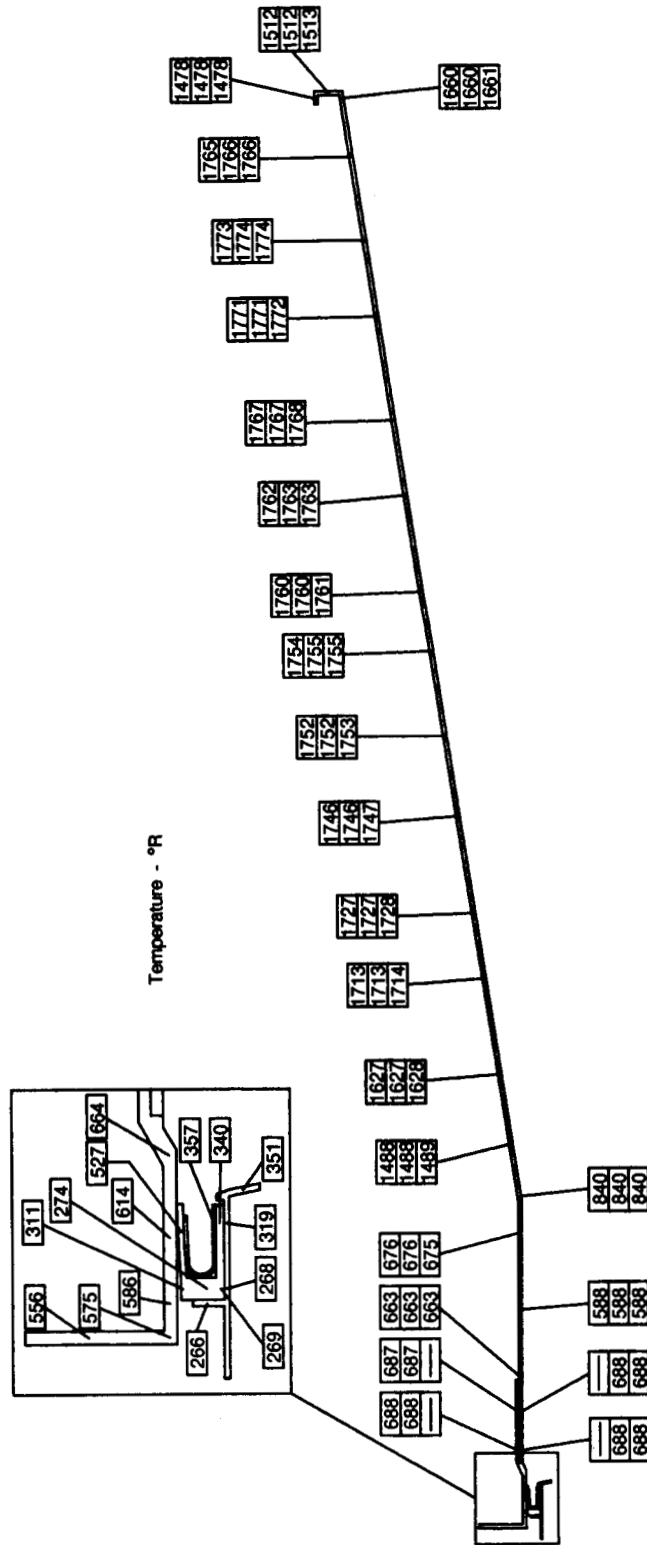
Figure 30. RL10A-3-3A 20-inch Cb Nozzle, O/F = 5.0, Thrust = 16.5K

FD 329929

38

3097C

SECTION VI
COATING SELECTION

The coating evaluation and selection process for the flight weight 20-inch columbium nozzle was divided into two phases. The first phase consisted of the laboratory evaluation of several silicide and aluminide coating candidates and the selection of the most promising for further evaluation. The second phase consisted of exposing the selected candidates to the RL10 exhaust environment under actual engine operating conditions and conducting post-test evaluations of their effectiveness in protecting the columbium substrate.

A. LABORATORY EVALUATION OF SELECTED COLUMBIUM COATING SAMPLES

After a literature search and an evaluation of the coating industry capability and experience in coating columbium alloys, two basic coating groups, aluminides and silicides were identified as potential coatings for the 20-inch columbium nozzle application. The vendor selection process was based on the guidelines in Table VI-1. Those vendors who could meet the guidelines were supplied with 0.015-inch thick, 4-inch by 6-inch, C-103 columbium test panels.

Table VI-1. *Guidelines For Selection of Coating Vendors*

• The coating would be vendor applied and fully developed
• The vendor must possess equipment and facilities capable of coating the large diameter (71 inch) nozzles
• The vendor shall apply a 3.0 ± 1.0 mil coating to test panels for screening evaluation
• The test panels will be tested in the engine environment by attachment to an RL10 nozzle during test firing

2784C

Upon receiving the coated panels, the coating candidates underwent microstructural and chemical reviews. The reviews included visual inspections, coating distribution and coating composition. Table VI-2 shows a ranking of the candidate coating quality, based primarily on metallographic determination of coating thickness, edge coverage and uniformity of microstructure.

The three silicide coatings (R512-E, VH-109, and W3-MOD) have the best general coating integrity and would appear to have the highest possibility of acceptable performance. The performance of the next two aluminides would depend greatly on the temperature ranges encountered by the panels. VH-2 (slurry applied Al) should perform well at intermediate temperatures (1000°F-1650°F) and R505-F (Sn matrix) should perform well at low temperatures (<1000°F). Attack at panel edges could be a problem for both of these coatings, considering the uniformity of the coating in these regions. The microstructure of VH-9 is interesting, but the inconsistent coating thickness and its unpredictable effect on substrate thickness make application of this coating on thin sheet difficult to control to specs. Improved thickness control of this coating would be required to consider it for the flight nozzle. No conclusions could be made about the suitability of RT-40; composition and microstructure of the panels received from the vendor were not consistent with specified processing of this coating.

Table VI-2. Relative Ranking of the Evaluated Coating Candidates

	Coating	Application Technique	Type/Constituents	Comments	Vendor
1.	R512-E	Slurry	Silicide Si, Cr, Fe	Excellent integrity	Hi Temp Co
2.	VH-109	Slurry	Silicide Si, Cr, Hf, Zn, Fe	Excellent integrity Slightly thicker than required	Vac Hyd
3.	W3-MOD	CVD	Silicide Si	Excellent integrity One-half of thickness required	Chromalloy
4.	VH-2	Slurry	Aluminide Al	Questionable structural integrity-"pull-out" Incomplete coating coverage at sample edges	Vac Hyd
5.	R505-F	Slurry	Aluminide Al, Zn, Mo	Questionable structural integrity-"Bubbles or pull-out" Nearly incomplete coating coverage at sample edges	Hi Tem Co
6.	VH-9	Slurry	Aluminide Al, Ti	Unique layered coating profile Radical thickness variations — coating and substrate Significant substrate consumption during coating process Unexpected detection of Si and Cr	Vac Hyd
7.	RT-40	CVD/Pack	Aluminide Al, Si	No Al in coating Coating origin unknown Coating thickness is well under design goal	Chromalloy

2784C

Based on the laboratory evaluation, the silicide coatings were selected to proceed to the engine test phase of the coating selection process. Preference was given to the R512-E and VH-109 coatings since they are both applied as a slurry, which makes them considerably less expensive than the CVD applied W3-MOD coating.

B. PHASE II. ENGINE TEST AND POST-TEST EVALUATION OF SELECTED COLUMBIUM COATING SAMPLES

Phase I of this study analyzed and ranked seven different coatings in the as-received condition from three vendors. The resultant rankings were based on the integrity and consistency of the coating. The most highly ranked coatings were R512-E from Hitemco and VH-109 from Vac Hyd. Columbium C-103 panels coated with R512-E and VH-109 and an uncoated C-103 panel were fixtured to an RL10 engine and exposed to the engine exhaust during engine firings to simulate the environment that a nozzle extension for such an engine would experience.

The three columbium samples were attached to the exit plane of the RL10 cyrogenically cooled nozzle and aligned with the I.D. surface of the engine nozzle. The samples were located equidistant from each other for symmetry. The test was initiated with an uncoated C-103 panel, an R512-E coated C-103 panel, and an VH-109 coated C-103 panel. The uncoated panel experienced excessive warping, cracking, and oxidation at 1203 seconds and six start/stop cycles into the testing sequence. It was removed and replaced by a nickel-based superalloy sample. The coated samples were tested through the entire testing sequence, accumulating 4451 seconds and 23 stop/start cycles.

Upon completion of the tests, the samples were removed from the engines and sent to the laboratory where they underwent microphotographic documentation, microstructural observations, microhardness measurements, and evaluation of the coating substrate thickness distribution. Additionally, columbium substrate specimens were removed from each of the samples and tested by a Leco gas analyser. The gas analysis determined the amount of O, H and N remaining in the substrate material of the three columbium samples.

Reduced substrate cross-sectional thickness was the primary difference between the performance of the coatings (Table VI-3). The observation that additional substrate may have been consumed by the VH-109 coating and the redistribution of secondary phases indicates that VH-109 may not be totally stable in this temperature range. The panel thickness varied from 13.5 mils at the inlet and exit planes to 10.1 mils at the panel center. The R512-E panel thickness was relatively constant at 13.3 mils. Data presented by Battelle-Columbus as part of this nozzle study (Ref. 5) concurred with the greater predictability of the R512-E over the VH-109. The predictability of the coating/substrate system interaction is critical. An unexpected deviation in the load-bearing cross-sectional area of the nozzle could result in an overload condition.

Table VI-3. *Average Coating and Panel Thickness at Various Locations of the R512-E and VH-109 Coated Panels*

		Average Panel Thickness	Average Chamber Side Coating	Average Gas Path Side Coating
R512E	Loc. 1	14.4	4.6	4.4
	3	13.3	4.6	4.2
	4	13.2	4.3	4.1
	5	13.4	4.5	4.4
	6	13.2	4.6	4.5
VH109	Loc. 1	13.5	6.0	5.0
	3	11.5	5.1	4.3
	4	10.1	4.7	4.0
	5	10.1	4.4	4.0
	6	13.5	6.0	5.6

2784C

To assist in understanding the role that oxygen takes in the RL10 environment, thermodynamic data was used to calculate the partial pressure of oxygen in the exhaust products and the partial pressure of oxygen required for the formation of oxides of columbium and silicon. The calculations were performed at three temperatures 298°K, 1144°K, and 1450°K. The maximum temperature was obtained from thermocouple measurements taken from a nickel-based alloy that was tested in a manner similar to the C-103 panels.

This theoretical analysis determined that the RL10 exhaust environment will favor Cb_2O_5 and SiO_2 formation at 1144°K. Table VI-4 compiles similar P_{o2} calculations at 298°K and 1450°K in addition to 1144°K. Although the RL10 produces a hydrogen-rich exhaust, there is enough oxygen in equilibrium with the exhaust products to allow the formation of the aforementioned oxides at all predicted operating temperatures. These findings document the need for a columbium protective coating in the RL10 application and the effectiveness of silicide as this coating.

Table VI-4. *Partial Pressure of Oxygen in Equilibrium with Water, Columbium Pentoxide, and Silicon Dioxide at 298°K, 1144°K, and 1450°K*

Temperature (°K)	(°F)	H_2 P_{o2}	Cb_2O_5 P_{o2}	SiO_2 P_{o2}
298	77	7.9×10^{-80}	$<1 \times 10^{-100}$	$<1 \times 10^{-100}$
1144	1600	1.4×10^{-16}	9.1×10^{-27}	7.6×10^{-33}
1450	2150	9.2×10^{-12}	1.3×10^{-19}	3.7×10^{-24}

2784C

Therefore, based on the above results, R512-E was selected as the best coating candidate for the RL10 columbium nozzle extension. It protected the substrate from significant O_2 embrittlement. It retained its original thickness and did not consume additional substrate material during the thermal exposure. It has a history of being applied to prescribed thickness consistently.

Although no deleterious effects of H_2 were detected by this investigation, an important aspect of reusable operation could not be included. Upon shutdown in low earth orbit, the nozzle would be expected to cool to cyrogenic temperatures. With the hydrogen absorbed during the firing to orbit, hydride precipitation in the C-103 alloy may occur. This may compromise mechanical properties of the substrate that are required for succeeding firings. Incorporation of a low temperature exposure should be included in the flight weight nozzle testing.

For a more complete description of the flight weight 20-inch columbium nozzle coating evaluation effort please refer to one of the following sources

1. P&W Internal Documents

    a. P&W Government Products Division Materials Development Laboratory Report No. 27272 "RL10 Radiantly Cooled Columbium Nozzle Extension Coating Screening Effort" 18 October 1985, K.S. Murphy

    b. P&W Government Products Division Materials Development Laboratory Report No. 28198 "RL10 Radiantly Cooled Columbium Nozzle Extension Coating Screening Effort Engine Test Results" 22 August 1986, K.S. Murphy

2. P&W Report FR 87-TBD
    NASA Report CR-TBD

    Coating Evaluation and Selection for a Flight Weight Columbium Nozzle for the RL10 Rocket Engine.

SECTION VII
CONCLUDING REMARKS

The design and analysis of the flight weight 20-inch columbium nozzle and the flight weight nozzle support seal and latching hardware for the RL10 rocket engine have been completed. The nozzle, nozzle seal, nozzle latching and nozzle support hardware will add 47.3 lb to the RL10 rocket engine. Fabrication of this hardware is underway. Two columbium nozzles will be fabricated by PSM/Fan Steel (Los Angeles, CA). The nozzles will be coated by HiTempCo (New York) with their proprietary R512-E silicide slurry coating.

The hardware fabrication will be completed during the first half of 1987. The hardware will be delivered to P&W where it will be installed in an RL10 engine and undergo testing during the summer of 1987. The results of this testing will be used to evaluate the suitability of columbium as a nozzle extension material for upper stage LOX/hydrogen rocket engines.

REFERENCES

1. Design & Analysis Report for the 20-Inch Carbon/Carbon Secondary Nozzle for the RL10 Engine, December, 1984. UTC Pratt & Whitney Report FR-18357-2. NASA Report CR-174859, J. H. Castro.

2. Summary of Carbon/Carbon Nozzle Testing on the RL10 Liquid Rocket Engine, Focusing on Results of Failure Analysis from Failed LPI Densified Nozzle, November, 1985. J.H. Castro, T.E. Blase; U.T.C. Pratt & Whitney presented at the 1985 JANNAF Rocket Nozzle Technology meeting in Monterey, California

3. Spec No. 2289A, 11 April 1985 "Model Specification Rocket Engine, Liquid Propellant; Pratt & Whitney RL10A-3-3A Atlas/Centaur and Shuttle Centaur applications.

4. Combustor Liner Film Cooling in the Presence of High Free Stream Turbulence; NASA TN D.-6360, July 1971, Juhasz, A.J. and Marek, C.J.

5. RL10 Nozzle Study Final Task Report; Contract Number NASW-3595 to NASA Headquarters - Office Code MS, 12 December 1985. Compiled by Ellis Foster, Battelle, Columbus Division

0076j

APPENDIX A
LATCH DENSITY STUDY

This section presents the results of a study to assess the effects of the number of latches on nozzle stresses and deflections. It also compares NASTRAN vs shell deck results.

There was concern that approximating the discrete latches in the shell deck with a modified property full hoop element might produce questionable results.

The results would become more questionable as the number of latches is reduced. Therefore a NASTRAN analysis was made of the secondary nozzle with each latch modeled (Figure 31). This was then compared to a shell deck analysis where properties in the latch region were modified to reflect the number of latches. Cases for 6, 12, 24 and 36 latches were run. Comparison of results between NASTRAN and the shell deck showed good agreement in stress but poor agreement in deflections.
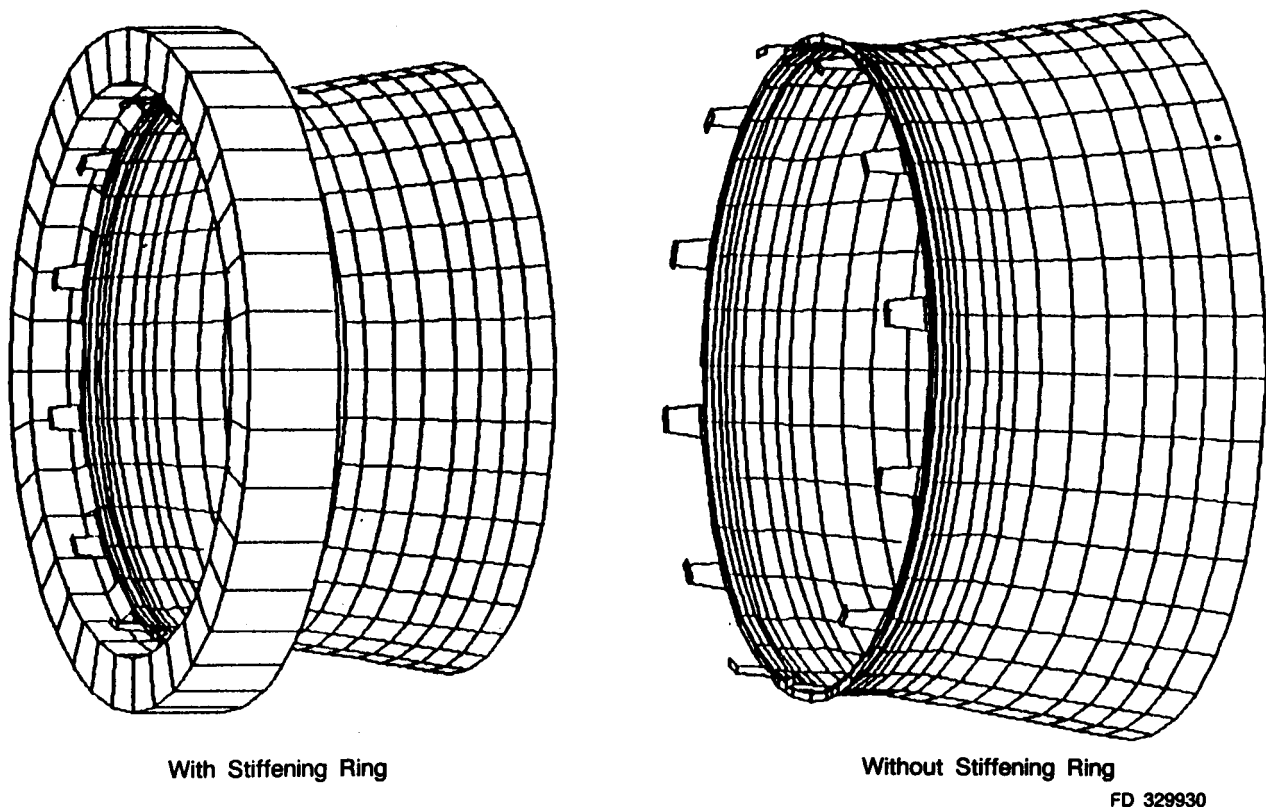

With Stiffening Ring   Without Stiffening Ring

FD 329930

Figure 31. NASTRAN Model for Latch Density Study

Figures 32 and 33 compare NASTRAN vs shell deck stresses for 12 and 24-latch cases respectively. There is general agreement in both cases although the NASTRAN results suffer from a coarse breakup necessitated by the large plate element model. The shell deck on the other hand can have many more axisymmetric elements to produce a finer definition of the stress variation as shown in Figures 32 and 33. Away from the latches it appears that the shell deck stresses are better, picking up for example, the compressive hoop stress spike that must arise at the cone-cylinder intersection; this was missed in the NASTRAN. NASTRAN, on the other hand, is probably somewhat better in the vicinity of the discrete latches; note in Figure 32 that the characteristic of the NASTRAN stress distribution is starting to diverge from the shell deck stress distribution near the latches.
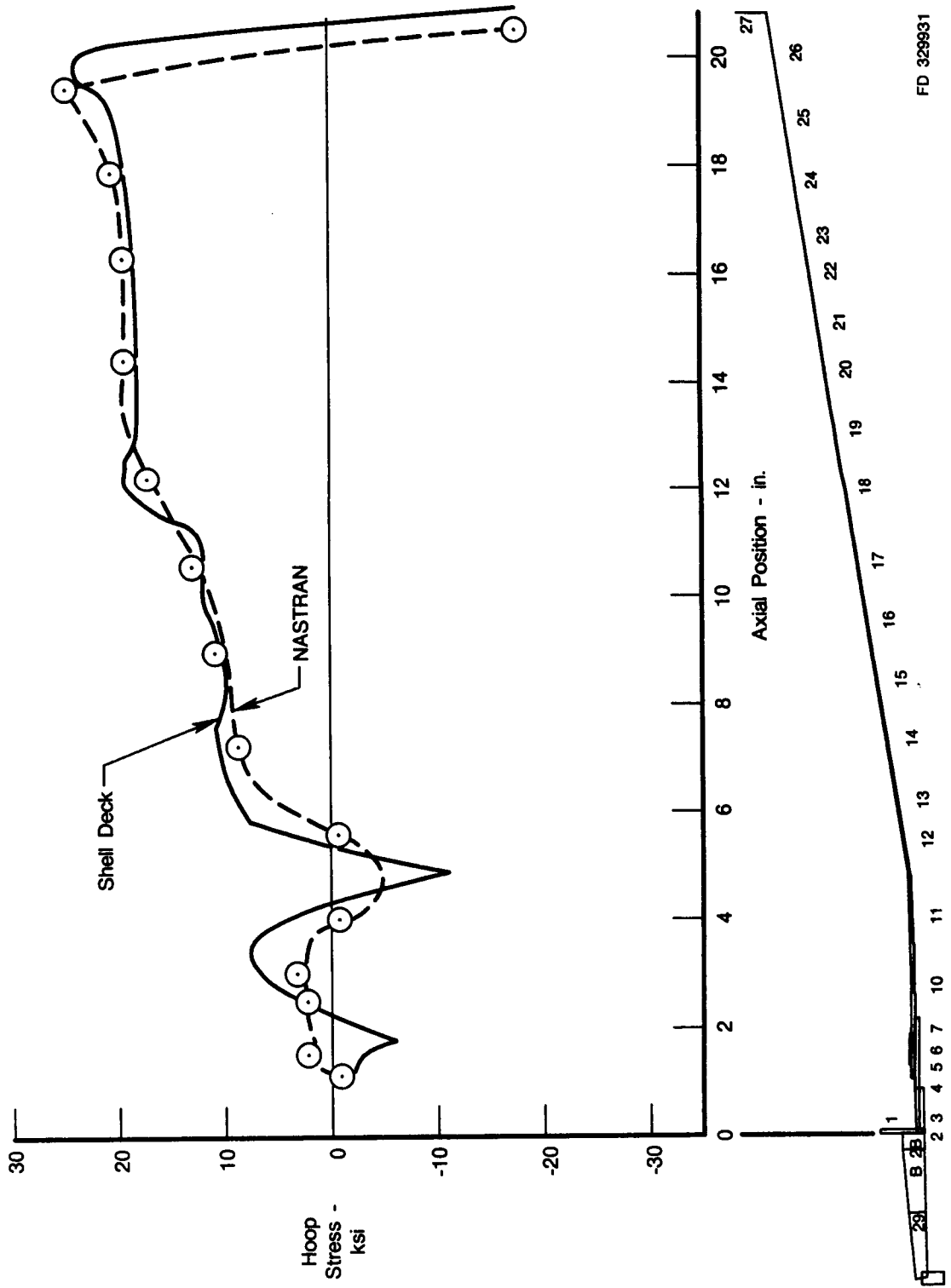
Figure 32. Comparison of NASTRAN vs Shell Deck Stresses at 0° O.D. Surface for 12 Latches and Test Stand Shutdown Loading

FD 329931
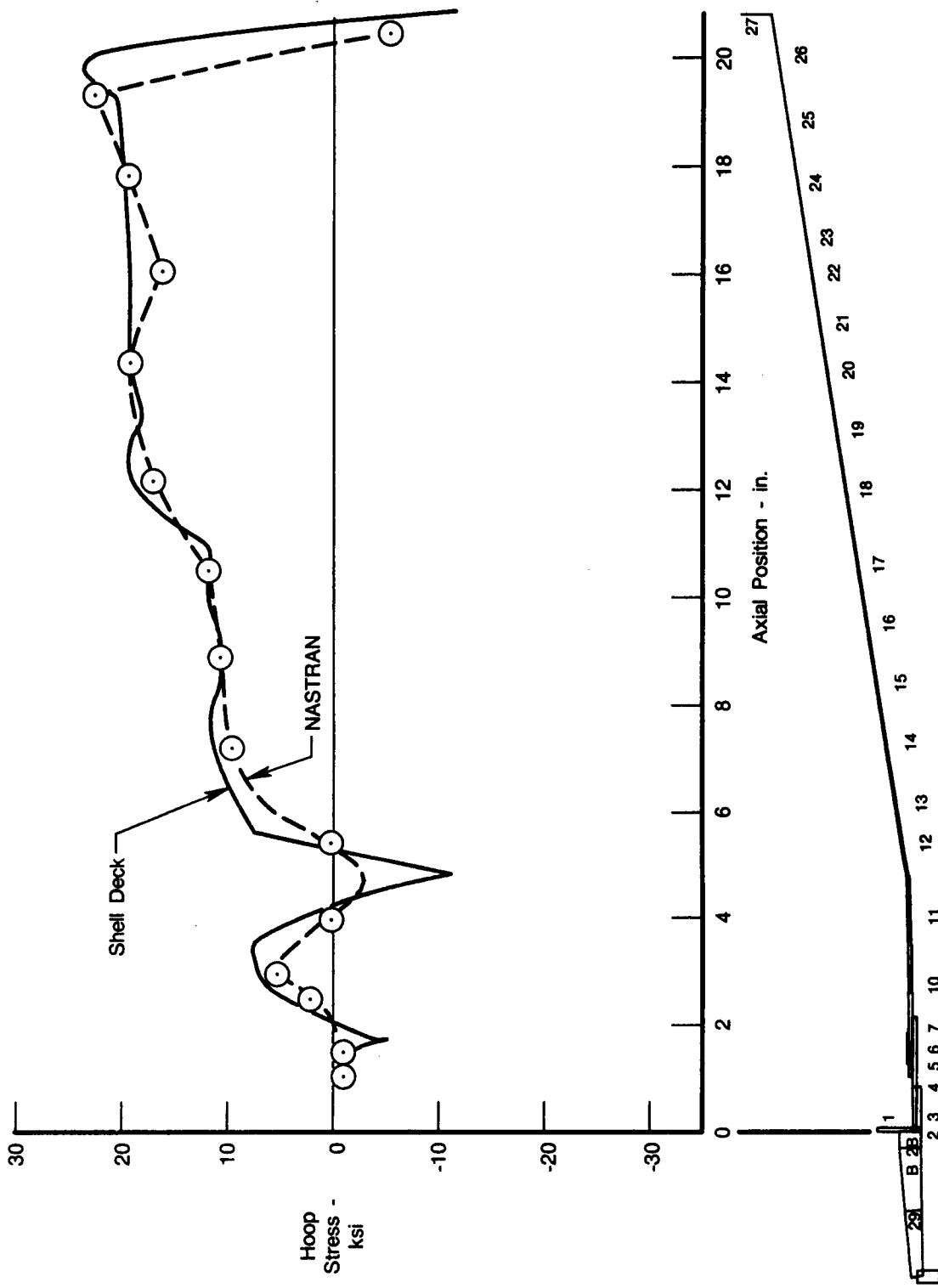
A-2

Figure 33. Comparison of NASTRAN vs Shell Deck Stresses at 0° O.D. Surface for 24 Latches and Test Stand Shutdown Loading

FDA 329632

A-3

There is generally poor agreement between NASTRAN and shell deck deflections as shown in Figure 34. Part of this discrepancy may be due to the NASTRAN approximation of a continuous shell structure with discrete plate elements and part may be due to the shell deck approximating discrete latches with a continuous shell element. Agreement is particularly poor for the 12-latch case without the removable stiffening ring. The agreement is better when the removable stiffening ring is part of the structure.
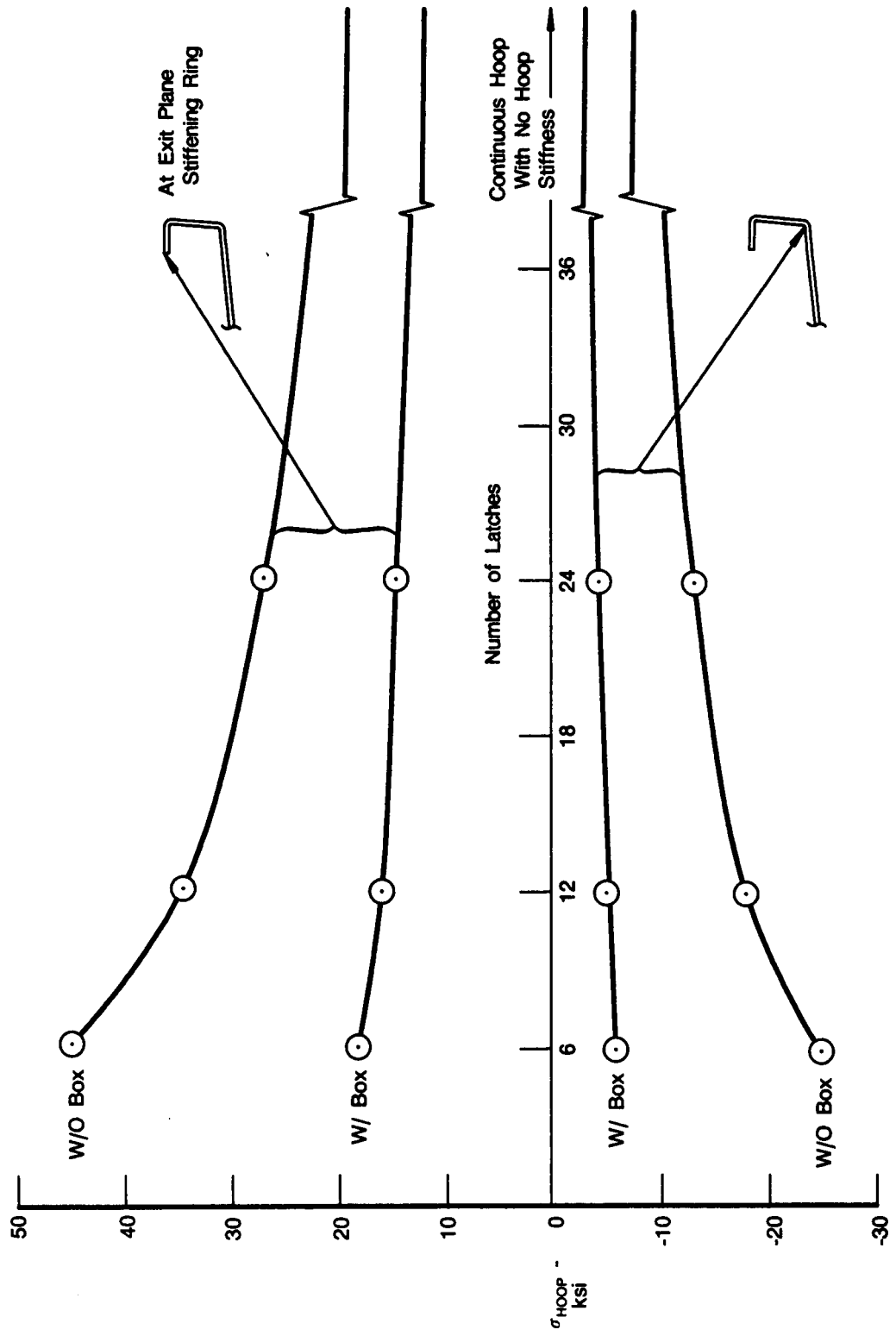
The stiffening ring makes the nozzle deflections and stresses insensitive to the number of latches as shown in Figures 34 and 35. It does this by functioning like a filter, absorbing much of the harmonic component of the shutdown load before it can be taken out by the latches.

Because stresses are the main criteria on which the columbium nozzle design is based and because the NASTRAN stresses tend to backup the shell deck stresses, the shell analysis was considered valid for the 12-latch design.
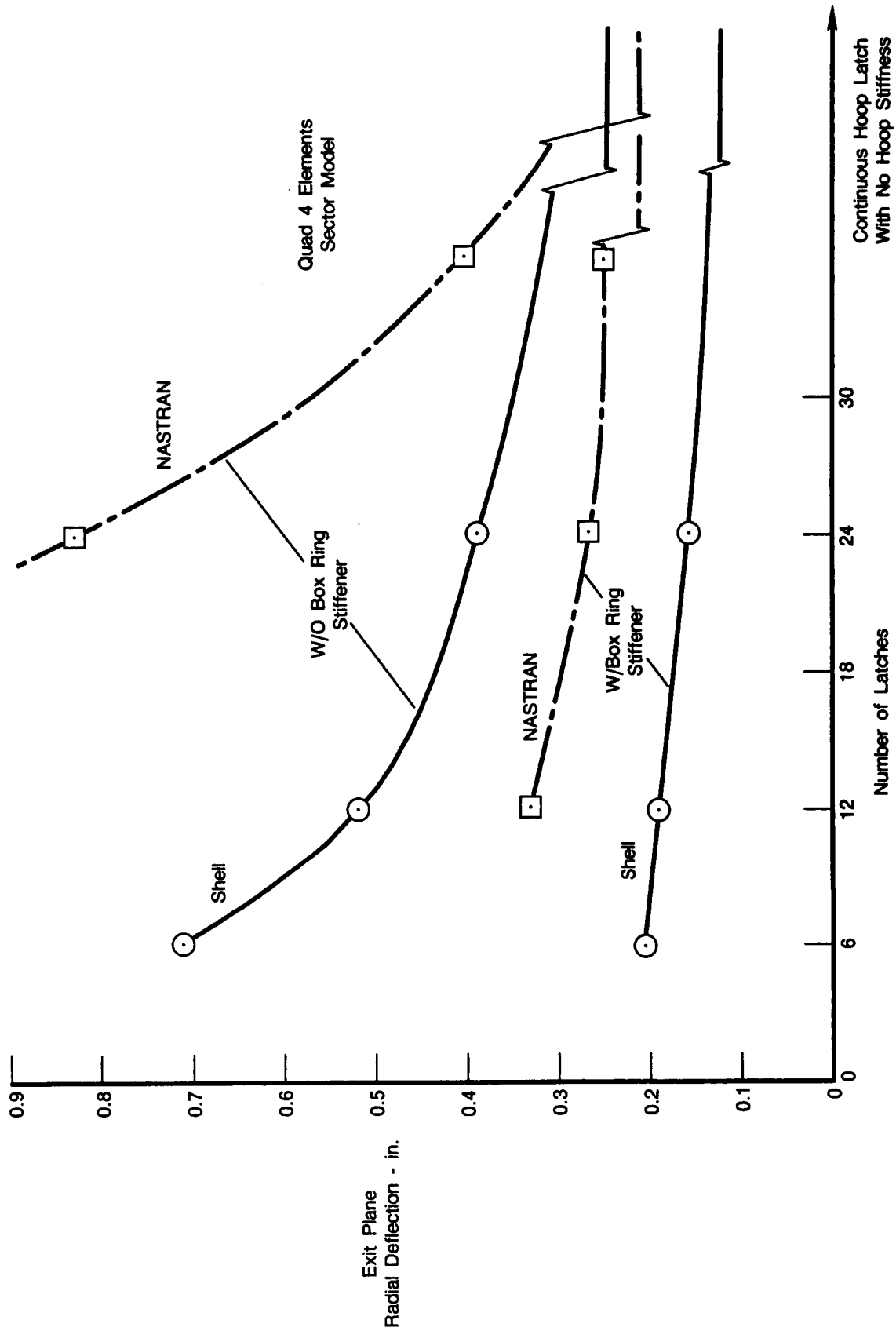
Figure 34. Cb Nozzle Latch Density Study for Test Stand Shutdown Loading

A-5

Figure 35. Cb Nozzle Latch Density Study — Shell Deck Results for Test Stand Shutdown Loading

A-6

1. Report No. CR-179612	2. Government Accession No.	3. Recipient's Catalog No.
4. Title and Subtitle Design and Analysis Report For The Flight Weight 20-Inch Columbium Secondary Nozzle For The RL10 Engine		5. Report Date March 1987
		6. Performing Organization Code
7. Author(s) Mr. J.H. Castro		8. Performing Organization Report No. FR-19692
9. Performing Organization Name and Address Pratt & Whitney P.O. Box 109600 West Palm Beach, FL 33410-9600		10. Work Unit No.
		11. Contract or Grant No. NAS3-24238
12. Sponsoring Agency Name and Address NASA Lewis Research Center 21000 Brookpark Road Cleveland Ohio, 44135		13. Type of Report and Period Covered Topical Report
		14. Sponsoring Agency Code

15. Supplementary Notes

Program Technical Monitor: R.L. DeWitt, NASA Lewis Research Center, Cleve., OH
Program Manager: J.A. Burkhart, NASA Lewis Research Center, Cleve., OH

16. Abstract

Pratt & Whitney (P&W) is currently under contract to NASA-LeRC for a multi-year program to evaluate the feasibility of the RL10-IIB/IIC engine models and the various improvements which broaden the engine capabilities and range of applications. The features being evaluated include the operation of the RL10 engine at low thrust levels and/or high mixture ratio levels and the addition of a high area ratio (250:1) translating nozzle to the engine to increase its specific impulse while shortening the installed engine length. The translating nozzle for the RL10-IIB/IIC engine is approximately 55 inches length with an exit plane diameter of 71 inches and an inlet plane diameter of 40 inches.

This report documents the design and analysis work done investigating a small subscale Columbium nozzle which could be built and tested to provide findings which then could be incorporated into the high area ratio nozzle final design for the RL10-IIB/IIC engine. The length of the subscale nozzle is 20 inches; its exit diameter is 46 inches. With the nozzle in the stowed position, an RL10A-3-3A engine system is 70 inches long (Area Ratio = 61:1); with the nozzle deployed the engine length and area ratio are increased to 90 inches and 83:1 respectively. The increase in area ratio provides a calculated increase of 7 ± 1 seconds of specific impulse.

17. Key Words (Suggested by Author(s)) Space Propulsion Systems Hydrogen/Oxygen Engine Expander Cycle Engines Secondary Nozzles Variable Thrust Rockets Liquid Propellant Rockets	18. Distribution Statement General Release		
19. Security Classif. (of this report) Unclassified	20. Security Classif. (of this page) Unclassified	21. No. of Pages 57	22. Price*

*For sale by the National Technical Information Service, Springfield, Virginia 22161